

Numerical analysis for leaky-integrate-fire networks under Euler–Maruyama

Xu'an Dou, Frank Chen, Kevin K Lin, Zhuo-Cheng Xiao*

March 12, 2026

* zx555@nyu.edu

Abstract

Leaky integrate-and-fire (LIF) networks are canonical reduced models for spike generation and synaptic filtering in computational neuroscience, and they are also a standard substrate for neuromorphic AI. We study time-driven Euler–Maruyama simulation of such networks with exponential synapses and instantaneous resets. Because diffusion acts only through the synaptic current and not directly on the voltage, each spike is a threshold hit for a deterministically advected voltage with random crossing speed. The numerical difficulty is therefore concentrated at event times: pathwise error is governed by spike-time error and by grid-induced spike-count mismatches.

For layered feedforward networks we prove finite-horizon mean-square strong bounds and weak order-one bounds for smooth bounded observables. The strong analysis uses a pruning-and-balance strategy. We split path space into a good set, where exact and numerical spike histories match and every matched spike has crossing speed $A = I - I_{\text{th}} \geq \alpha$, and a bad set containing near-tangential crossings and the terminal mismatch layer. On the good set, spike-time error is controlled by the local Euler–Maruyama error multiplied by A^{-1} . A threshold-flux estimate then yields the logarithmic truncated inverse-moment bound

$$\mathbb{E}[A^{-2} \mathbb{1}_{\{A \geq \alpha\}}] \lesssim \alpha_0^{-2} + T \rho_{\max} \log(\alpha_0/\alpha),$$

while near-tangential events have probability $O(T\alpha^2)$. Choosing $\alpha = \alpha(h)$ to balance the good- and bad-set contributions gives mean-square error h times polylogarithmic factors, with explicit dependence on depth, time, and weight norms. Hence, away from the spike-count mismatch near the observation horizon, the strong behavior matches the classical Euler–Maruyama 1/2 rate up to logarithmic losses.

For weak error we adapt a semigroup/backward-Kolmogorov argument to the reset map. The one-step defect splits into an interior Taylor term and a boundary-strip probability-flow term controlling missed and extra spikes, which yields global order 1, $O(Th)$. We also derive a Lyapunov exponent formula coupling the stationary threshold flux to the reset saltation factor, and we outline deterministic and noisy recurrent extensions, including loop-truncated strong bounds governed by synaptic cycles and rate/density controls. The resulting trajectory-level theory separates single-trial spike-time fidelity from observable-level accuracy, making it relevant both for mechanistic neuroscience models and for neuromorphic AI systems that compute through sparse events and filtered readouts.

Contents

1	Introduction	3
1.1	Motivation: why spiking resets change numerical analysis	3
1.2	Related work	4
1.3	Contributions and interpretation	4
1.4	Notation	6
1.5	Organization	7

2	Feedforward current-based LIF network and EM scheme	7
2.1	Architecture, state variables, and spike trains	7
2.2	Continuous-time dynamics with reset	7
2.3	Euler–Maruyama scheme with grid-based threshold/reset	8
2.4	Spike-time error (STE)	9
2.5	Main results	9
3	Strong error via spike-time analysis	10
3.1	Warm-up: strong error when noise is injected directly into the voltage	10
3.2	Single-neuron strong STE bound (noise enters I only)	12
3.3	The quadratic small tangency-bad set	14
3.4	A conservative explicit estimate of ρ_{\max}	15
3.5	Spike-count mismatch bad set (sharp)	16
3.6	Propagation of spike-time errors across feedforward layers	18
3.6.1	Synaptic kernel and the misalignment window	18
3.6.2	L_t^1 current perturbation induced by presynaptic STE	19
3.6.3	Voltage perturbation is Lipschitz in L_t^1 current perturbation	19
3.6.4	Layerwise STE recursion (explicit constants)	20
3.7	Network strong error bound via pruning	20
3.7.1	Network good/bad events	20
3.7.2	Pruning decomposition	21
3.7.3	Bounding the bad probability (explicit α and T dependence)	21
3.7.4	Iterating the STE recursion	21
3.7.5	A strong MSE bound explicit in T , L , and weights	21
3.7.6	Interpretation: depth and time growth in the pruning bound	22
3.8	When depth does not deteriorate the strong exponent	23
3.8.1	No intrinsic noise downstream	23
4	Weak error: order 1 with explicit dependence on depth, time, and weights	24
4.1	State space, spike maps, and the exact Markov semigroup	25
4.2	EM one-step operator	25
4.3	Backward value function and transmission at threshold	25
4.4	Quantities controlling the weak constant	26
4.5	Two core lemmas: timing/decay vs. missed/extra spikes	26
4.6	One-step and global weak error bounds	27
5	Dynamical stability and Lyapunov exponents	28
5.1	Common-noise coupling and what “stability” means	28
5.2	Warm-up: deterministic 1D IF with common input	29
5.2.1	Model and spike times	29
5.2.2	Order preservation and contraction between spikes	29
5.2.3	Monotonicity and (mean-driven) Lipschitz bounds for spike times	29
5.2.4	Interlacing and spike-count mismatch is at most one	30
5.2.5	Spike-count bounds from input integrals	31
5.3	A general 1D IF Lyapunov exponent theorem	31
5.3.1	Stochastic IF with autonomous input	31
5.3.2	Invariant measure and boundary flux	32
5.4	Single current-based LIF neuron: explicit λ and bounds	33
5.5	Feedforward networks: upstream exponents force downstream divergence	34
5.5.1	A forcing estimate: spike-time divergence \Rightarrow current divergence	34
5.5.2	A max-rule for layerwise Lyapunov exponents	34
5.6	Implications for strong error accumulation in time	35

6	Recurrent networks: intuition and strong error bounds	36
6.1	Intuition: recurrence creates an effective depth through feedback loops	36
6.2	Model: recurrent current-based LIF network	36
6.3	Scenario 1: deterministic mean-driven recurrent hybrid system ($\sigma \equiv 0$)	36
6.3.1	Continuous variational flow	36
6.3.2	Saltation matrix at a spike event	37
6.3.3	Hybrid fundamental matrix and a Lyapunov upper bound	37
6.3.4	Mean-driven deterministic numerics: error growth controlled by λ_{hyb}	38
6.4	Scenario 2: noisy recurrent networks under rate and density bounds	39
6.4.1	Rate bounds and synchrony control	39
6.4.2	Boundary density constants and their estimates	39
6.4.3	Tangency probability and spike-count mismatch probability	40
6.4.4	Good-set STE inequality and explicit loop-length truncation	41
6.4.5	Pruning strong bound for noisy recurrent networks	43
7	Recurrent networks: weak error under rate and density bounds	45
7.1	Spike maps and a weight norm for recurrent jumps	45
7.2	Rate bounds and second factorial moment	45
7.3	One-step weak defect: explicit dependence on R_{net} and $R_{\text{net},2}$	45
7.4	Global weak order 1 with explicit rate dependence	46
8	Discussion	47

1 Introduction

1.1 Motivation: why spiking resets change numerical analysis

Leaky integrate & fire (LIF) networks occupy an unusual position. They are among the simplest models that retain spike timing, synaptic filtering, and reset dynamics, so they are ubiquitous in computational neuroscience [6, 12]. At the same time, the same event-driven structure makes LIF-type units natural building blocks for neuromorphic hardware and spike-based artificial intelligence, where sparse spikes are used for temporal processing, online adaptation, and energy-efficient computation [17, 18, 20, 21, 25, 26]. In both settings, the central numerical question is not only whether a discretization approximates the continuous state, but also whether it preserves the correct spike train, firing statistics, and downstream synaptic effects.

This distinction matters because different scientific questions probe different notions of accuracy. In neuroscience modeling, pathwise accuracy matters when one studies precise spike timing, synchrony, spike-triggered plasticity, or reliability under common input; weak accuracy matters when the targets are firing rates, smooth readouts, or other averaged statistics. In neuromorphic computation, the same split appears as temporal fidelity of event streams versus accuracy of network-level functionals accumulated from those streams [5, 11, 24]. A numerical theory that separates these regimes is therefore useful beyond the immediate mathematical setting.

Spiking neuron models are hybrid systems: continuous subthreshold evolution is punctuated by synaptic jumps and an instantaneous voltage reset [6, 12]. In LIF models the only nonlinearity is the threshold/reset rule, so discretization error is largely an event-resolution problem. Standard SDE convergence theory, usually formulated for globally Lipschitz coefficients or for jumps at prescribed times, does not directly capture missed spikes, delayed spikes, or reset-induced propagation of timing error; see the simulation literature [14, 15, 23, 27].

We study current-based LIF networks with temporally exponential synaptic kernels, discretized by Euler–Maruyama (EM). Because the voltage has no direct diffusion, a spike is a boundary hit for an advected voltage with random crossing speed $A = I - I_{\text{th}}$. In fluctuation-driven regimes A

can be arbitrarily small. This forces a spike-time analysis, replaces the usual globally Lipschitz perturbation picture by a transversality problem at threshold, and produces logarithmic losses in strong error bounds. We start from a layered feedforward architecture, then extend our results to recurrent spiking networks.

1.2 Related work

Spiking models in neuroscience and neuromorphic computation. Integrate-and-fire models have long served as reduced descriptions of neural excitability, fluctuation-driven spiking, and synaptic integration [12]. They also sit at the core of neuromorphic engineering, from Mead’s original event-based vision [21] to silicon neuron circuits, large spiking chips, and modern spike-based AI [9, 17, 22, 25, 26]. This breadth of use makes numerical fidelity a shared issue: the same simulator may be used to test neural hypotheses, benchmark hardware mappings, or train and analyze spike-based models [11, 24].

Simulation algorithms and numerical pitfalls. Time-driven simulation of integrate-and-fire networks is standard but can miss spikes unless the time step is very small. Early analyses and practical remedies include [14, 27], as well as spike-time interpolation and exact subthreshold integration schemes [15, 23]. A broad survey is given in [6]. These works are primarily algorithmic or software-oriented; a finite-time strong/weak convergence theory for networks with threshold resets is still limited.

Mean-field and Fokker–Planck discretizations. A complementary literature develops structure-preserving schemes for the Fokker–Planck equations of noisy LIF models and their mean-field limits; see, e.g., [16]. These PDE schemes naturally address distributional evolution and firing-rate statistics, whereas the present work targets strong and weak error for time-discrete *trajectory* simulation of finite networks.

Exit times and boundary effects. At the single-neuron level, the spike time is a first-passage time. For diffusion-driven exits, Euler monitoring on a grid typically yields a $1/4$ strong exponent and requires boundary corrections for weak order one [1, 2, 13]. Our setting is degenerate: diffusion enters through I but not through v . The singular factor is the inverse crossing speed at threshold, whose truncated moments diverge only logarithmically under a boundary-flux bound. This leads to mean-square strong error of size h up to polylogarithmic factors, except for a terminal-time mismatch layer for discontinuous observables.

Dynamical stability and Lyapunov exponents in integrate-and-fire models. The stability of spike timing under common input is central both to neural reliability and to robust temporal computation [5, 20]. For deterministic one-dimensional spiking models, [4] expressed the Lyapunov exponent in terms of the spike map; in hybrid-systems language this is a saltation factor for the reset. For noise-driven oscillators, explicit Lyapunov formulas also arise in weak-noise phase reduction [28]. Here we adapt the saltation/flux perspective to the current-based (v, I) LIF neuron, describe how feedforward coupling propagates exponents across layers, and connect deterministic recurrent-network stability to numerical error growth via a hybrid fundamental matrix.

1.3 Contributions and interpretation

From a neuroscience viewpoint, the strong results concern single-trial spike-train fidelity, whereas the weak results concern averaged or smooth observables such as firing-rate readouts. From a neuromorphic-computation viewpoint, the same distinction separates event-stream accuracy from

correctness of network-level functionals. With this interpretation in mind, the main messages are as follows (proved in Sections 2–7):

- (i) **Strong error via spike times and pruning.** We analyze strong error for time-driven Euler–Maruyama (EM) in feedforward current-based LIF networks by coupling exact and numerical paths and pruning “bad” trajectories. On the good set, spike-time error (STE) is controlled by the local EM error multiplied by the inverse crossing speed $A = I - I_{\text{th}}$ at threshold. A boundary-flux argument shows (a) near-tangential spikes have probability $O(T\alpha^2)$ and (b) the truncated inverse moment grows only logarithmically: $\mathbb{E}[A^{-2}\mathbb{1}_{\{A \geq \alpha\}}] \lesssim \alpha_0^{-2} + T\rho_{\max} \log(\alpha_0/\alpha)$ ($\forall \alpha_0 > \alpha$). As a result, away from terminal-time spike-count mismatches, the squared strong error scales like h times polylogarithmic factors in h . Thus the pathwise behavior is “almost” the EM 1/2 rate, and the deviation from the textbook picture is traced to near-grazing threshold crossings rather than to bulk subthreshold EM error. We also quantify the grid-detection mismatch probability $\mathbb{P}(N^h(T) \neq N(T)) = O(\sqrt{h} \log(1/h))$; for discontinuous terminal observables this mismatch layer can dominate the pruning bound.
- (ii) **When depth does not change the strong h -exponent.** In noisy layers, the good-set recursion picks up one logarithmic inverse-moment factor per layer. If no intrinsic current noise enters layers $\ell \geq 2$ and downstream spikes have a deterministic transversality margin, then no new small-speed events are created downstream. The strong h -exponent is then inherited from layer 1, and depth affects only the constants through weights and spike counts. Thus synaptic depth can amplify error constants without necessarily changing the basic step-size exponent.
- (iii) **Weak error is order 1 with explicit constants.** We obtain global weak order 1 for spike-map compatible $\Phi \in C_b^4$ by a backward-Kolmogorov/Markov-operator argument that explicitly accounts for off-grid spikes. The one-step weak defect is $O(h^2)$ and decomposes into diffusion truncation, synaptic timing/decay, and missed/extra spike decisions. The spike-decision term is controlled by a boundary-strip probability-flow estimate; no “spike snapping” is assumed. The global error is $O(Th)$ with constants explicit in firing-rate bounds, synaptic time scales, and weight norms; under uniform rate/weight bounds the depth dependence is at most linear. This is the regime most directly relevant to smooth population-level readouts.
- (iv) **Dynamical stability and Lyapunov exponents.** For a single neuron driven by a stationary current we derive an explicit Lyapunov exponent formula combining the boundary flux of the stationary Fokker–Planck equation with the reset saltation factor; the threshold singularity is integrable. For feedforward networks the variational system is triangular, yielding a max-type propagation rule for Lyapunov exponents across layers. This links spike-timing reliability to numerical error amplification. We also explain how contraction can reduce long-time growth constants on good trajectories but cannot remove pruning contributions coming from missed spikes.
- (v) **Recurrent extensions.** For deterministic mean-driven recurrent networks we derive an explicit hybrid fundamental matrix, an upper bound on the hybrid Lyapunov exponent, and a quantitative link between λ_{hyb} and long-time discretization error growth. For noisy recurrent networks we give strong and weak error bounds under explicit rate moment bounds ($R_{\text{net}}, R_{\text{net},2}$) and boundary-density controls; on the strong good set, spike-time propagation admits a loop-length truncation in terms of the shortest directed cycle of the synaptic graph. These recurrent results identify graph cycles and recurrent gain as the natural quantities controlling long-time error growth in spike-based dynamical computation.

1.4 Notation

Table 1 collects the main notation used throughout the manuscript. Each symbol is defined at its first occurrence in the text; the table is intended as a quick reference.

Table 1: Notation used throughout the manuscript.

Symbol	Meaning
L	Feedforward depth (number of layers).
n_ℓ	Number of neurons in layer ℓ ; $N = \sum_{\ell=1}^L n_\ell$.
ℓ	Layer index ($1 \leq \ell \leq L$); i, j denote neuron indices within a layer.
\mathcal{I}	Index set of neurons: $\mathcal{I} = \{(\ell, j) : 1 \leq \ell \leq L, 1 \leq j \leq n_\ell\}$.
τ_v, τ_c	Voltage and synaptic-current time constants.
V_{th}, V_r	Voltage threshold and reset level ($V_r < V_{\text{th}}$).
I_{th}	Threshold current: $I_{\text{th}} = (V_{\text{th}} - V_r)/\tau_v$.
$v_{\ell,j}(t)$	Voltage of neuron (ℓ, j) at time t .
$I_{\ell,j}(t)$	Synaptic current of neuron (ℓ, j) at time t .
$b_{\ell,j}(t)$	Deterministic input (drift) in the current equation.
$\sigma_{\ell,j}$	Brownian noise amplitude in the current equation.
$B_{\ell,j}(t)$	Independent standard Brownian motions.
$W_{ji}^{\ell-1,\ell}$	Feedforward weight from presynaptic neuron $(\ell-1, i)$ to postsynaptic neuron (ℓ, j) .
$s_{\ell,j}^k$	k th exact spike time of neuron (ℓ, j) (upward threshold hit).
$N_{\ell,j}(t)$	Exact spike count up to time t : $N_{\ell,j}(t) = \sum_k \mathbf{1}_{\{s_{\ell,j}^k \leq t\}}$.
$A_{\ell,j}^k$	Threshold crossing speed at $s_{\ell,j}^k$: $A_{\ell,j}^k = I_{\ell,j}((s_{\ell,j}^k)^-) - I_{\text{th}}$.
h	Time step; $t_m = mh$ are grid times.
$\Delta B_{\ell,j,m}$	Brownian increment $B_{\ell,j}(t_{m+1}) - B_{\ell,j}(t_m) \sim \mathcal{N}(0, h)$.
$v_{\ell,j}^h(t_m), I_{\ell,j}^h(t_m)$	Numerical approximations at grid times (Euler / Euler–Maruyama).
$\hat{s}_{\ell,j}^k$	k th numerical spike time (grid-based detection).
$N_{\ell,j}^h(t)$	Numerical spike count up to time t .
$\Delta N_{\ell,j}^h(m)$	Numerical spikes of neuron (ℓ, j) in $[t_m, t_{m+1})$ (typically 0 or 1).
$\varepsilon_{\ell,j}^k$	Spike-time error (STE): $\varepsilon_{\ell,j}^k = \hat{s}_{\ell,j}^k - s_{\ell,j}^k$.
α	Transversality cutoff: crossings with $A < \alpha$ are declared (tangency-)bad.
α_0	Fixed upper cutoff for admissible α (technical; used in density bounds).
$B_{\ell,j}^{\text{tan}}(\alpha, T)$	Tangency-bad event up to horizon T : some spike has $A_{\ell,j}^k < \alpha$.
$B_{\ell,j}^{\text{mis}}(h, T)$	Mismatch-bad event (false positives): $N_{\ell,j}^h(T) > N_{\ell,j}(T)$.
$G_{\ell,j}(h, T; \alpha)$	Good event for neuron (ℓ, j) : complement of $B_{\ell,j}^{\text{tan}} \cup B_{\ell,j}^{\text{mis}}$.
$G_L(h, T; \alpha)$	Network-level good event: intersection of $G_{\ell,j}(h, T; \alpha)$ over all neurons.
$\Delta_\ell(T)$	Good-set RMS STE envelope at layer ℓ (defined via max over spikes up to T).
$C_{\ell,j}^{\text{loc}}(T)$	Subthreshold EM strong-error coefficient for neuron (ℓ, j) on $[0, T]$.
C_{max}	A (model-dependent) uniform bound used to control the strong error on the bad set (pruning).
$\Lambda_{\ell,j}(T)$	Spike-load bound (number of spikes of neuron (ℓ, j) up to T on the good set).
$\rho_{\text{max},\ell,j}(T, \alpha_0)$	Uniform bound on the joint density at threshold used in tangency probability estimates.
$\varrho_{\ell,j}^V(v, t)$	Voltage marginal density of $v_{\ell,j}(t)$.
$\rho_{\text{max},\ell,j}^V(T)$	Uniform bound on $\varrho_{\ell,j}^V$ in a unit strip below V_{th} (used for false positives and weak error).
$\mu_{\ell,j}(t), \sigma_{\text{eff},\ell,j}(t)$	Effective drift and diffusion in an OU surrogate for $I_{\ell,j}(t)$.
D	Interior state space for weak error: $D = \{x = (v, I) : v_{\ell,j} < V_{\text{th}} \forall (\ell, j)\}$.
Σ_p	Threshold surface for neuron p : $\Sigma_p = \{x \in \bar{D} : v_p = V_{\text{th}}\}$.
\mathcal{R}_p	Spike map (reset of v_p and synaptic jump(s) in postsynaptic currents).
$X(t)$	Exact Markov process on D with resets/jumps; $P_{s,t}$ is its semigroup.
Q_h	One-step EM Markov operator (grid spike-map composition).
$u(t, x)$	Backward value function $u(t, x) = (P_{t,T}\Phi)(x)$ for weak error analysis.

(continued on next page)

Symbol	Meaning
$R_\ell(T)$	Bound on expected number of spikes in layer ℓ per time step: $\mathbb{E}[\Delta N_\ell(m)] \leq R_\ell(T)h$.
$\ W^{\ell,\ell+1}\ _1$	Column-sum norm of a feedforward weight matrix (used in weak-error constants).
λ	Lyapunov exponent for common-noise synchronization/decoupling.
$\rho_\infty(V_{\text{th}}, I)$	Stationary boundary density (Fokker–Planck flux at threshold) used in λ .
$S(I)$	Saltation (reset) factor at a spike with current I (hybrid variational jump).
N_r	Number of neurons in a recurrent network.
W	Recurrent weight matrix; $\ W\ _1$ is its column-sum norm.
L^*	Length of the shortest directed synaptic cycle (take $L^* = \infty$ if the graph is acyclic).
$K_{\text{eff}}(T)$	Effective causal depth up to time T (maximal length of a time-ordered synaptic influence chain on the good set).
$G(T)$	Recurrent STE gain matrix with entries $G_{ij}(T) = \frac{2}{\alpha_i} W_{ij} \Lambda_j^{\text{rec}}(T)$.
$R_{\text{net}}(T)$	Network rate-moment bound: $\mathbb{E}[\Delta N_{\text{tot}}(m)] \leq R_{\text{net}}(T)h$ for total spikes $\Delta N_{\text{tot}}(m)$.
$R_{\text{net},2}(T)$	Second factorial-moment bound controlling within-step multi-spike probability: $\mathbb{E}[\Delta N_{\text{tot}}(m)(\Delta N_{\text{tot}}(m) - 1)] \leq R_{\text{net},2}(T)h^2$.

1.5 Organization

Section 2 introduces the model and EM discretization and summarizes the main results. Section 3 contains the STE-based strong analysis, including depth/time scaling and two regimes avoiding depth deterioration. Section 4 provides the weak order-1 proof with explicit constants. Section 5 derives Lyapunov exponents and their feedforward propagation, and discusses implications for long-time strong error. Sections 6–7 extend strong/weak bounds to recurrent networks under deterministic transversality and/or rate/density controls. The manuscript ends with a brief conclusion.

2 Feedforward current-based LIF network and EM scheme

2.1 Architecture, state variables, and spike trains

Fix a depth $L \geq 1$. Layer ℓ contains n_ℓ neurons. For neuron (ℓ, j) let $v_{\ell,j}(t)$ be voltage and $I_{\ell,j}(t)$ be synaptic current. Spike times $\{s_{\ell,j}^k\}_{k \geq 1}$ are successive threshold hits (we use the left limit because v is reset at spikes):

$$s_{\ell,j}^1 := \inf\{t > 0 : v_{\ell,j}(t^-) = V_{\text{th}}\}, \quad s_{\ell,j}^{k+1} := \inf\{t > s_{\ell,j}^k : v_{\ell,j}(t^-) = V_{\text{th}}\}.$$

The counting process is $N_{\ell,j}(t) = \sum_{k \geq 1} \mathbb{1}_{\{s_{\ell,j}^k \leq t\}}$.

2.2 Continuous-time dynamics with reset

Fix $\tau_v, \tau_c > 0$ and reset level $V_r < V_{\text{th}}$. Between spikes of neuron (ℓ, j) :

$$dv_{\ell,j}(t) = \left(-\frac{1}{\tau_v} (v_{\ell,j}(t) - V_r) + I_{\ell,j}(t) \right) dt, \quad v_{\ell,j}(t) < V_{\text{th}}, \quad (1)$$

$$dI_{\ell,j}(t) = -\frac{1}{\tau_c} (I_{\ell,j}(t) - b_{\ell,j}(t)) dt + \frac{\sigma_{\ell,j}}{\tau_c} dB_{\ell,j}(t) + \sum_{i=1}^{n_{\ell-1}} W_{ji}^{\ell-1,\ell} dN_{\ell-1,i}(t), \quad \ell \geq 2, \quad (2)$$

and for $\ell = 1$ the sum over i is replaced by external input only (equivalently take $W^{0,1} \equiv 0$). Here $\{B_{\ell,j}\}$ are independent standard Brownian motions, and $b_{\ell,j}(t)$ are bounded deterministic inputs.

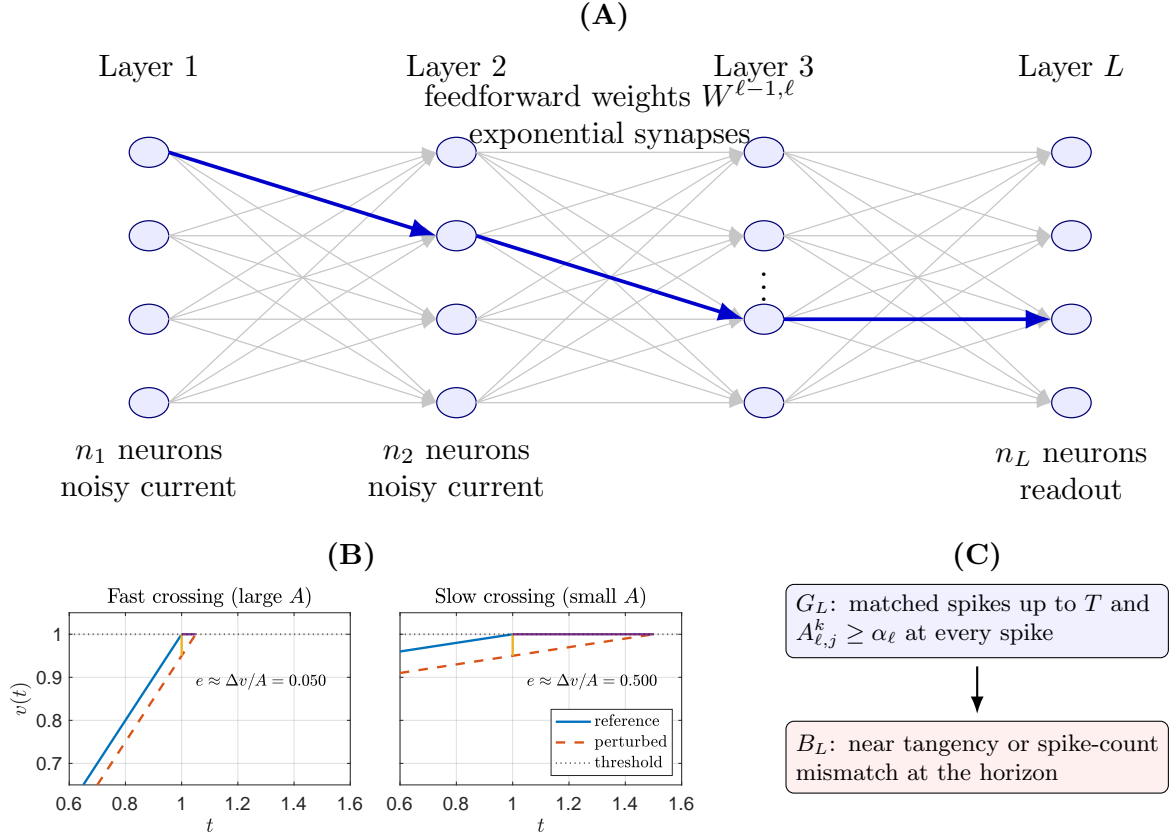


Figure 1: A feedforward network architecture and strong error proof strategy. **(A)** Feedforward network architecture with noisy currents in every layer, feedforward weights $W^{\ell-1,\ell}$, and temporally exponential synaptic kernel. **(B)** Illustration of fast and slow threshold crossings. Blue: true solution (reference); red: numerical solution (perturbed); yellow: pathwise error (Δv); purple: spike time error (e_m). **(C)** Pruning decomposition of the mean-square strong error into a good set G_L and a bad set B_L .

When $v_{\ell,j}$ hits V_{th} from below at time $s_{\ell,j}^k$, it resets instantly:

$$v_{\ell,j}((s_{\ell,j}^k)^-) = V_{\text{th}} \quad \Rightarrow \quad v_{\ell,j}((s_{\ell,j}^k)^+) = V_{\text{r}}, \quad I_{\ell,j} \text{ is continuous at } s_{\ell,j}^k. \quad (3)$$

Remark 2.1 (Threshold current and crossing speed). Define the threshold current

$$I_{\text{th}} := \frac{V_{\text{th}} - V_{\text{r}}}{\tau_{\text{v}}}.$$

At a spike time $s = s_{\ell,j}^k$, the instantaneous upward crossing speed equals

$$A_{\ell,j}^k := \dot{v}_{\ell,j}(s^-) = -\frac{1}{\tau_{\text{v}}}(V_{\text{th}} - V_{\text{r}}) + I_{\ell,j}(s^-) = I_{\ell,j}(s^-) - I_{\text{th}}. \quad (4)$$

Necessarily $A_{\ell,j}^k > 0$ at a genuine upward crossing, but it can be arbitrarily small in fluctuation-driven regimes.

2.3 Euler–Maruyama scheme with grid-based threshold/reset

Fix $h > 0$ and grid $t_m := mh$. Let $\Delta B_{\ell,j,m} = B_{\ell,j}(t_{m+1}) - B_{\ell,j}(t_m) \sim \mathcal{N}(0, h)$.

Current update.

$$I_{\ell,j}^h(t_{m+1}) = I_{\ell,j}^h(t_m) - \frac{h}{\tau_c} (I_{\ell,j}^h(t_m) - b_{\ell,j}(t_m)) + \frac{\sigma_{\ell,j}}{\tau_c} \Delta B_{\ell,j,m} + \sum_{i=1}^{n_{\ell-1}} W_{ji}^{\ell-1,\ell} \Delta N_{\ell-1,i}^h(m), \quad (5)$$

where $\Delta N_{\ell-1,i}^h(m) \in \{0, 1\}$ indicates whether the numerical presynaptic neuron $(\ell - 1, i)$ fired in $[t_m, t_{m+1})$.

Voltage update and spike detection.

$$v_{\ell,j}^h(t_{m+1}) = v_{\ell,j}^h(t_m) + h \left(-\frac{1}{\tau_v} (v_{\ell,j}^h(t_m) - V_r) + I_{\ell,j}^h(t_m) \right). \quad (6)$$

If $v_{\ell,j}^h(t_{m+1}) \geq V_{\text{th}}$, we register a numerical spike at $\hat{s}_{\ell,j}^k := t_{m+1}$ and reset $v_{\ell,j}^h(t_{m+1}) \leftarrow V_r$. Let $N_{\ell,j}^h(t)$ be the corresponding numerical spike count.

Continuous-time interpolation. When we write $(v_{\ell,j}^h(t), I_{\ell,j}^h(t))$ for t between grid points, we mean the standard continuous-time EM interpolation on each step (coefficients frozen at t_m and driven by the same Brownian path); this is the version used in sup-norm bounds and in the spike-time sensitivity estimate below.

2.4 Spike-time error (STE)

When exact and numerical spike sequences can be matched in order up to time T , define

$$\varepsilon_{\ell,j}^k := \hat{s}_{\ell,j}^k - s_{\ell,j}^k, \quad s_{\ell,j}^k \leq T. \quad (7)$$

2.5 Main results

For SIAM-style readability, we summarize the main results here; full assumptions, constants, and proofs appear in Sections 3–7.

Theorem (Strong error (pruning bound; “almost” 1/2 rate)). Fix $T > 0$ and let $X_L(T)$ be a bounded network output functional that is Lipschitz in the layer- L spike-time metric on the good set (Section 3.7.5). Assume the boundary-density bound (14), the voltage strip bound (57), Assumption 3.23, and the STE tail hypothesis used in Lemma 3.16. For any truncation thresholds $\alpha_1, \dots, \alpha_L \in (0, \alpha_0]$, there exist explicit constants such that

$$\begin{aligned} & \mathbb{E} \left[\left\| X_L^h(T) - X_L(T) \right\|^2 \right] \\ & \leq \text{Lip}_X^2 \Delta_L(T)^2 + C_{\max}^2 \left(C_{\text{mis}}(T) \sqrt{h \log(1/h)} + \frac{T}{2} \sum_{\ell=1}^L \sum_{j=1}^{n_\ell} \rho_{\max,\ell,j}(T, \alpha_0) \alpha_\ell^2 \right), \end{aligned}$$

where $\Delta_L(T)$ satisfies the STE recursion (41) (equivalently the explicit form (44)) with logarithmic inverse-speed factors from Lemma 3.8. Balancing the good-set term with the tangency mass (and ignoring the terminal-time mismatch layer) gives mean-square error of order h times polylogarithmic factors in h , hence an “almost” Euler–Maruyama 1/2 strong rate for spike-time controlled observables.

Theorem (Weak error (order one)). Let $T = Mh$ and $\Phi \in C_b^4(\mathbb{D})$ be spike-map compatible at the terminal time T . Under the regularity/rate assumptions in Section 4,

$$\left| \mathbb{E}[\Phi(X(T))] - \mathbb{E}[\Phi(X^h(T))] \right| \leq Th C_{\text{weak}}(T, L, W),$$

with an explicit constant $C_{\text{weak}}(T, L, W)$ given in (65). Under uniform rate and weight bounds, C_{weak} grows at most linearly in the depth L .

Theorem (Lyapunov exponents (saltation/flux and feedforward propagation)). In a stationary regime with boundary flux $J_\infty(I) = (I - I_{\text{th}})\rho_\infty(V_{\text{th}}, I)\mathbb{1}_{\{I > I_{\text{th}}\}}$, the top Lyapunov exponent of a single neuron under common-noise coupling is

$$\lambda = -\frac{1}{\tau_v} + \int_{\mathbb{R}} J_\infty(I) \log\left(\frac{I}{I - I_{\text{th}}}\right) dI,$$

and the logarithmic singularity at $I \downarrow I_{\text{th}}$ is integrable. For feedforward networks, conditional on matched spike trains, layerwise exponents satisfy the max-rule $\lambda_\ell = \max\{\lambda_\ell^{\text{diag}}, \lambda_{\ell-1}\}$ for $\ell \geq 2$.

Theorem (Recurrent extensions (deterministic and noisy)). For deterministic recurrent networks in a mean-driven (uniformly transversal) regime, the hybrid fundamental matrix admits the explicit product form (94) and the top hybrid Lyapunov exponent satisfies the explicit upper bound in Theorem 6.2. Moreover, for the time-driven Euler scheme with grid reset, deterministic global discretization error and STE grow at most like $e^{\lambda_{\text{hyb}}T}$ (Theorem 6.5), so $\lambda_{\text{hyb}} < 0$ yields uniform-in- T $O(h)$ accuracy while $\lambda_{\text{hyb}} > 0$ implies exponential-in- T error amplification at rate at most λ_{hyb} .

For noisy recurrent networks, under rate moment bounds $(R_{\text{net}}, R_{\text{net},2})$ and boundary density controls $(\rho_{\text{max}}, \rho_{\text{max}}^V)$, we obtain pruning-type strong error bounds; on the strong good set, STE propagation admits an explicit loop-length truncation governed by the shortest directed cycle length of the synaptic graph (Theorem 6.13). Weak error remains order 1 with constants depending explicitly on $R_{\text{net}}, R_{\text{net},2}$ and $\|W\|_1$ (Theorem 7.2).

3 Strong error via spike-time analysis

Throughout, strong error is controlled by spike-time mismatches and a pruning good/bad split. The technical core is: (i) quantify probability of near-tangential crossings $A < \alpha$, and (ii) propagate spike-time perturbations across layers while accounting for synaptic jump misalignment.

3.1 Warm-up: strong error when noise is injected directly into the voltage

This warm-up is included to emphasize the key intuition used throughout the strong analysis. Consider a single LIF neuron with *voltage diffusion*:

$$dv(t) = \left(-\frac{1}{\tau_v}(v(t) - V_r) + \bar{I}\right) dt + \sigma_v dB(t), \quad v(t) < V_{\text{th}}, \quad (8)$$

with instantaneous reset $v(s^-) = V_{\text{th}} \Rightarrow v(s^+) = V_r$. Let $\{s^k\}$ be spike times and $N(t)$ the spike count.

Discretize by Euler–Maruyama with grid $t_m = mh$:

$$v^h(t_{m+1}) = v^h(t_m) + h\left(-\frac{1}{\tau_v}(v^h(t_m) - V_r) + \bar{I}\right) + \sigma_v \Delta B_m, \quad \Delta B_m \sim \mathcal{N}(0, h), \quad (9)$$

and if $v^h(t_{m+1}) \geq V_{\text{th}}$ we register a numerical spike at t_{m+1} and reset $v^h(t_{m+1}) \leftarrow V_r$.

Intuition. Away from threshold, the coefficients are smooth and EM behaves as for a standard SDE: the strong error scales like $h^{1/2}$ in RMS. An $\mathcal{O}(1)$ discrepancy can only be created if the exact and numerical trajectories *disagree about a spike*, because a spike triggers the discontinuous reset $v \mapsto V_r$. Thus “bad things” only happen at (or very near) spike times; the strong analysis reduces to quantifying the probability of a one-step spike decision mismatch.

Theorem 3.1 (Warm-up: pruning strong bound for voltage-noise LIF). *Fix $T > 0$ and couple the exact and numerical schemes by using the same Brownian increments. Let $e_m := v^h(t_m) - v(t_m)$ and let $B^{\text{mis}}(h, T)$ be the event that there exists a time step in which exactly one of $\{v, v^h\}$ registers a spike. Then there exists $C(T)$ such that*

$$\mathbb{E}\left[\sup_{m:t_m \leq T} |e_m|^2\right] \leq C(T)h + C_{\text{max}}^2 \mathbb{P}(B^{\text{mis}}(h, T)), \quad (10)$$

where C_{max} is a deterministic bound on $|e_m|$ after a mismatch (e.g. $C_{\text{max}} \leq V_{\text{th}} - V_r$). Moreover, in fluctuation-driven regimes (no uniform transversality at threshold), $\mathbb{P}(B^{\text{mis}}(h, T)) = \mathcal{O}(Th^{1/2})$, so the pruning bound yields

$$\mathbb{E}\left[\sup_{m:t_m \leq T} |e_m|^2\right] \lesssim Th^{1/2}, \quad \text{i.e. RMS order at least } h^{1/4}.$$

In mean-driven regimes with a deterministic transversality margin, $\mathbb{P}(B^{\text{mis}}(h, T)) = 0$ for h sufficiently small, and the classical RMS order $h^{1/2}$ is recovered.

Proof. For each grid step $[t_m, t_{m+1}]$ define the exact and numerical spike indicators

$$S_m := \mathbb{1}_{\{\exists s \in (t_m, t_{m+1}]: v(s^-) = V_{\text{th}}\}}, \quad \hat{S}_m := \mathbb{1}_{\{v^h(t_{m+1}^-) \geq V_{\text{th}}\}}.$$

Then the mismatch event can be written as

$$B^{\text{mis}}(h, T) = \bigcup_{m: t_{m+1} \leq T} \{S_m \neq \hat{S}_m\} = \bigcup_{m: t_{m+1} \leq T} (\{S_m = 1, \hat{S}_m = 0\} \cup \{S_m = 0, \hat{S}_m = 1\}).$$

Let $G^{\text{mis}}(h, T) := (B^{\text{mis}}(h, T))^c$.

Step 1: good-set case decomposition (“no spike” vs. “both spike”). On $G^{\text{mis}}(h, T)$, the spike decision agrees step-by-step, so for each m with $t_{m+1} \leq T$ we are in exactly one of the two cases:

(i) *No spike in the step:* $S_m = \hat{S}_m = 0$.

(ii) *Both spike in the step:* $S_m = \hat{S}_m = 1$ (exact spikes at some $s \in (t_m, t_{m+1}]$ and the numerical scheme spikes at t_{m+1}).

Step 2: strong error on G^{mis} (standard EM away from threshold). In case (i), there is no reset in the step for either trajectory, and both follow the same scalar OU SDE (8) driven by the same Brownian increment. Standard EM strong estimates for globally Lipschitz SDEs yield a one-step mean-square defect $\mathcal{O}(h^2)$ and hence, after summation over m , the bound

$$\mathbb{E}\left[\sup_{m: t_m \leq T} |e_m|^2 \mathbb{1}_{G^{\text{mis}}}\right] \leq C(T)h \quad (\text{case (i), aggregated over steps}).$$

In case (ii), both trajectories are reset to V_r at the same grid time t_{m+1} , so the reset itself does not amplify the discrepancy. The pre-reset error is again controlled by the same OU EM estimate on an interval of length at most h , and after the common reset the error is bounded by the same quantity. Thus the same $C(T)h$ estimate holds when summing over the (random) set of spike steps on G^{mis} .

Step 3: “one spikes” \Rightarrow pruning. On the bad set $B^{\text{mis}}(h, T)$ there exists a first step m_* on which $S_{m_*} \neq \hat{S}_{m_*}$, so exactly one of the two trajectories is reset. This can create an $\mathcal{O}(1)$ discrepancy immediately. Rather than attempting a pathwise “catch-up” coupling after the first disagreement, we prune: we bound $|e_m| \leq C_{\max}$ deterministically for all subsequent times, where one may take $C_{\max} \leq V_{\text{th}} - V_r$.

Therefore,

$$\mathbb{E}\left[\sup_{m: t_m \leq T} |e_m|^2\right] \leq \mathbb{E}\left[\sup_{m: t_m \leq T} |e_m|^2 \mathbb{1}_{G^{\text{mis}}}\right] + C_{\max}^2 \mathbb{P}(B^{\text{mis}}(h, T)) \leq C(T)h + C_{\max}^2 \mathbb{P}(B^{\text{mis}}(h, T)),$$

which is (10).

Step 4: scaling of $\mathbb{P}(B^{\text{mis}}(h, T))$. In mean-driven regimes (uniform positive drift at threshold), one-step spike decisions are stable: for h small enough, a transversal exact crossing forces $v(t_{m+1}) \geq V_{\text{th}}$ whenever a spike occurs in the step, and similarly the numerical crossing cannot occur without an exact crossing; hence $\mathbb{P}(B^{\text{mis}}(h, T)) = 0$.

In fluctuation-driven regimes, v has Brownian diffusion, so it can hit V_{th} and return below it before the next grid point. This is precisely the classical “grid monitoring” exit-time error mechanism. Standard boundary-layer estimates for Euler schemes imply $\mathbb{P}(B^{\text{mis}}(h, T)) \leq CT h^{1/2}$ (see, e.g., [1, 2]), completing the proof. \square

Remark 3.2 (How is this warm-up example related to current-noise LIF). For the current-based model studied below, v has no diffusion. Therefore the “Brownian recrossing” mechanism behind the $O(Th^{1/2})$ mismatch probability in the warm-up disappears. Instead, the dominant strong obstruction becomes *near-tangential crossings* (small A), whose probability is governed by the boundary flux (13) and scales like $O(T\alpha^2)$. False-positive numerical spikes remain possible (numerical fires but exact does not), but we show their probability is still only $O(Th^{1/2})$ under a mild voltage-density bound and is subleading in the depth recursion for $L \geq 2$ (Lemma 3.16 and Remark 3.18).

From now on, we return to the analysis of current-noise LIF neurons in Eq. (1) and (2). We state a robust L^2 spike-time estimate that does not assume a deterministic transversality margin. The strategy is to divide the full path space into a “good” and a “bad” set, where the good set not only exclude spiking mismatch but also truncate in threshold-crossing speed α .

3.2 Single-neuron strong STE bound (noise enters I only)

Good/bad events and the refined mismatch set. Fix $T > 0$ and $\alpha \in (0, \alpha_0]$. Define the tangency-bad event

$$B_{\ell, j}^{\text{tan}}(\alpha, T) := \{\exists k : s_{\ell, j}^k \leq T \text{ and } A_{\ell, j}^k < \alpha\}, \quad G_{\ell, j}^{\text{tan}}(\alpha, T) := (B_{\ell, j}^{\text{tan}}(\alpha, T))^c.$$

Mismatch event (spike-count mismatch at the horizon). To avoid the overly pessimistic “prune-after-the-first step mismatch” strategy, we define mismatch as a *spike-count* discrepancy on the observation horizon:

$$B_{\ell, j}^{\text{mis}}(h, T) := \{N_{\ell, j}^h(T) \neq N_{\ell, j}(T)\}. \quad (11)$$

This definition is symmetric (extra or missed spikes) and, crucially, it *does not* declare a trajectory bad merely because a spike is advanced/delayed by a small amount and the spike counts differ

on a short intermediate time interval. On $(B_{\ell,j}^{\text{mis}}(h, T))^c$, the spike trains up to time T can be paired by index: the k th numerical spike time $\hat{s}_{\ell,j}^k$ corresponds to the k th exact spike time $s_{\ell,j}^k$ for $k = 1, \dots, N_{\ell,j}(T)$.

Define the full bad event and its complement:

$$B_{\ell,j}(h, T; \alpha) := B_{\ell,j}^{\text{tan}}(\alpha, T) \cup B_{\ell,j}^{\text{mis}}(h, T), \quad G_{\ell,j}(h, T; \alpha) := B_{\ell,j}(h, T; \alpha)^c.$$

Remark 3.3 (On the α - h roles in the good/bad split). In earlier stepwise “grid monitoring” analyses, one often absorbs missed spikes into the tangency-bad set, which requires a compatibility condition linking the grid size to the transversality margin (e.g. $h \ll \alpha^2$ for coarse endpoint-detection schemes). In the present section we avoid this restriction by defining mismatch via the *spike-count* discrepancy $N^h(T) \neq N(T)$, whose probability is bounded sharply in Section 3.5. The cutoff α is therefore used only to control the geometric singularity A^{-1} in the spike-time sensitivity; thanks to the log-truncated inverse-moment estimate, the good-set strong error depends on α only through $-\log \alpha$ (cf. Lemma 3.8).

Lemma 3.4 (Transversal sensitivity: STE is controlled by voltage error and the crossing speed). *Fix a neuron (ℓ, j) and let $s_{\ell,j}^k$ be an exact spike time and $\hat{s}_{\ell,j}^k$ the matched numerical spike time produced by the grid-based detection rule. Write $\varepsilon_{\ell,j}^k := \hat{s}_{\ell,j}^k - s_{\ell,j}^k$ and define the crossing speed*

$$A_{\ell,j}^k := \dot{v}_{\ell,j}((s_{\ell,j}^k)^-) = -\frac{1}{\tau_v}(V_{\text{th}} - V_r) + I_{\ell,j}((s_{\ell,j}^k)^-) = I_{\ell,j}((s_{\ell,j}^k)^-) - I_{\text{th}}.$$

Assume $A_{\ell,j}^k > 0$ and that the matching occurs within one time step, i.e. $\hat{s}_{\ell,j}^k \in (s_{\ell,j}^k - h, s_{\ell,j}^k + h]$. Then, for h small enough,

$$\left| \varepsilon_{\ell,j}^k \right| \leq h + \frac{2}{A_{\ell,j}^k} \sup_{t \in [s_{\ell,j}^k - h, s_{\ell,j}^k + h]} \left| v_{\ell,j}(t) - v_{\ell,j}^h(t) \right|. \quad (12)$$

Proof. Because $A_{\ell,j}^k > 0$ and $I_{\ell,j}$ is continuous between spikes, for h small enough the exact voltage is strictly increasing on $[s_{\ell,j}^k - h, s_{\ell,j}^k + h]$ and satisfies $\dot{v}_{\ell,j}(t) \geq A_{\ell,j}^k/2$ there. Let $\hat{s} := \hat{s}_{\ell,j}^k$ and let $\tilde{s} \in [\hat{s} - h, \hat{s}]$ be the (within-step) threshold time of the continuous-time EM interpolation, so that $v_{\ell,j}^h(\tilde{s}) = V_{\text{th}}$ and $|\hat{s} - \tilde{s}| \leq h$. Since $v_{\ell,j}((s_{\ell,j}^k)^-) = V_{\text{th}}$, we have

$$0 = v_{\ell,j}^h(\tilde{s}) - v_{\ell,j}((s_{\ell,j}^k)^-) = (v_{\ell,j}^h(\tilde{s}) - v_{\ell,j}(\tilde{s})) + (v_{\ell,j}(\tilde{s}) - v_{\ell,j}((s_{\ell,j}^k)^-)).$$

The first term is bounded by $\sup_{t \in [s_{\ell,j}^k - h, s_{\ell,j}^k + h]} |v_{\ell,j}(t) - v_{\ell,j}^h(t)|$. For the second term, the mean value theorem and $\dot{v}_{\ell,j} \geq A_{\ell,j}^k/2$ give $|v_{\ell,j}(\tilde{s}) - v_{\ell,j}((s_{\ell,j}^k)^-)| \geq (A_{\ell,j}^k/2) |\tilde{s} - s_{\ell,j}^k|$. Hence

$$\left| \tilde{s} - s_{\ell,j}^k \right| \leq \frac{2}{A_{\ell,j}^k} \sup_{t \in [s_{\ell,j}^k - h, s_{\ell,j}^k + h]} \left| v_{\ell,j}(t) - v_{\ell,j}^h(t) \right|.$$

Finally, $|\hat{s} - s_{\ell,j}^k| \leq |\hat{s} - \tilde{s}| + |\tilde{s} - s_{\ell,j}^k| \leq h + \dots$, which yields (12). \square

Lemma 3.5 (Subthreshold EM strong error for (v, I)). *Consider the coupled exact/EM solutions driven by the same Brownian path on an interval without spikes (so no reset). Then*

$$\mathbb{E} \left[\sup_{t \leq T} \left| I(t) - I^h(t) \right|^2 \right] \leq C_I(T) h, \quad \mathbb{E} \left[\sup_{t \leq T} \left| v(t) - v^h(t) \right|^2 \right] \leq C_v(T) h,$$

with $C_I(T), C_v(T)$ depending on τ_v, τ_c , coefficient bounds and T .

Proof. This is standard EM strong order 1/2 for the OU current SDE and linear stability for the voltage ODE driven by I ; see, e.g., [19]. \square

We comment that, the proof strategy for the strong error of single current-noise LIF neurons is that, we bound the probability of the bad set, and compute the strong error for trajectories in the good set.

3.3 The quadratic small tangency-bad set

Let $\rho_{\ell,j}(v, I, t)$ denote the subthreshold joint density of $(v_{\ell,j}(t), I_{\ell,j}(t))$ on $\{v < V_{\text{th}}\}$ (assume it exists and is sufficiently regular). Because there is no diffusion in v , the v -flux through the boundary requires a positive $(I - I_{\text{th}})$, and is purely advective:

$$J_{\ell,j}(I, t) = (I - I_{\text{th}}) \rho_{\ell,j}(V_{\text{th}}, I, t) \mathbb{1}_{\{I > I_{\text{th}}\}}. \quad (13)$$

Define the boundary-density bound

$$\rho_{\max,\ell,j}(T, \alpha_0) := \sup_{t \in [0, T]} \sup_{a \in [0, \alpha_0]} \rho_{\ell,j}(V_{\text{th}}, I_{\text{th}} + a, t). \quad (14)$$

Definition 3.6 (Near-tangency spike count). For $\alpha \in (0, \alpha_0]$ define the random count of near-tangential spikes by time T :

$$\mathcal{T}_{\ell,j}(\alpha, T) := \#\{k : s_{\ell,j}^k \leq T, A_{\ell,j}^k < \alpha\}.$$

Note that $B_{\ell,j}^{\text{tan}}(\alpha, T) = \{\mathcal{T}_{\ell,j}(\alpha, T) \geq 1\}$.

Lemma 3.7 (Expected number of near-tangential spikes is $O(T\alpha^2)$). Fix $\alpha \in (0, \alpha_0]$. Then

$$\mathbb{E}[\mathcal{T}_{\ell,j}(\alpha, T)] \leq \frac{T}{2} \rho_{\max,\ell,j}(T, \alpha_0) \alpha^2. \quad (15)$$

Consequently,

$$\mathbb{P}(B_{\ell,j}^{\text{tan}}(\alpha, T)) \leq \mathbb{E}[\mathcal{T}_{\ell,j}(\alpha, T)] \leq \frac{T}{2} \rho_{\max,\ell,j}(T, \alpha_0) \alpha^2. \quad (16)$$

Proof. By (13), the mean number of spikes with $A \in (0, \alpha)$ equals

$$\int_0^T \int_{I_{\text{th}}}^{I_{\text{th}} + \alpha} (I - I_{\text{th}}) \rho_{\ell,j}(V_{\text{th}}, I, t) dI dt = \int_0^T \int_0^\alpha a \rho_{\ell,j}(V_{\text{th}}, I_{\text{th}} + a, t) da dt \leq \frac{T}{2} \rho_{\max,\ell,j}(T, \alpha_0) \alpha^2,$$

proving (15). The probability bound follows from Markov inequality: $\mathbb{P}(\mathcal{T} \geq 1) \leq \mathbb{E}[\mathcal{T}]$. \square

Lemma 3.8 (Log-truncated inverse moment of the crossing speed). Fix $\alpha \in (0, \alpha_0]$ and consider any spike index k of neuron (ℓ, j) . Then

$$\mathbb{E} \left[\frac{1}{(A_{\ell,j}^k)^2} \mathbf{1}_{\{s_{\ell,j}^k \leq T, \alpha \leq A_{\ell,j}^k \leq \alpha_0\}} \right] \leq T \rho_{\max,\ell,j}(T, \alpha_0) \log \frac{\alpha_0}{\alpha}. \quad (17)$$

Consequently,

$$\mathbb{E} \left[\frac{1}{(A_{\ell,j}^k)^2} \mathbf{1}_{\{s_{\ell,j}^k \leq T, A_{\ell,j}^k \geq \alpha\}} \right] \leq \frac{1}{\alpha^2} + T \rho_{\max,\ell,j}(T, \alpha_0) \log \frac{\alpha_0}{\alpha}. \quad (18)$$

Proof. Since the integrands are nonnegative, for every sample path we have the pointwise domination

$$\frac{1}{(A_{\ell,j}^k)^2} \mathbf{1}_{\{s_{\ell,j}^k \leq T, \alpha \leq A_{\ell,j}^k \leq \alpha_0\}} \leq \sum_{m: s_{\ell,j}^m \leq T} \frac{1}{(A_{\ell,j}^m)^2} \mathbf{1}_{\{\alpha \leq A_{\ell,j}^m \leq \alpha_0\}}.$$

Taking expectations and using the flux identity (13) with the test function $\phi(a) = a^{-2} \mathbf{1}_{\{\alpha \leq a \leq \alpha_0\}}$ gives

$$\begin{aligned} \mathbb{E} \left[\frac{1}{(A_{\ell,j}^k)^2} \mathbf{1}_{\{s_{\ell,j}^k \leq T, \alpha \leq A_{\ell,j}^k \leq \alpha_0\}} \right] &\leq \mathbb{E} \left[\sum_{m: s_{\ell,j}^m \leq T} \frac{1}{(A_{\ell,j}^m)^2} \mathbf{1}_{\{\alpha \leq A_{\ell,j}^m \leq \alpha_0\}} \right] \\ &= \int_0^T \int_\alpha^{\alpha_0} \frac{1}{a^2} a \rho_{\ell,j}(V_{\text{th}}, I_{\text{th}} + a, t) da dt \\ &\leq T \rho_{\max,\ell,j}(T, \alpha_0) \int_\alpha^{\alpha_0} \frac{1}{a} da = T \rho_{\max,\ell,j}(T, \alpha_0) \log \frac{\alpha_0}{\alpha}, \end{aligned}$$

which is (17). For (18), split the event $\{A_{\ell,j}^k \geq \alpha\}$ into $\{\alpha \leq A_{\ell,j}^k \leq \alpha_0\} \cup \{A_{\ell,j}^k > \alpha_0\}$ and use $A_{\ell,j}^k > \alpha_0 \Rightarrow (A_{\ell,j}^k)^{-2} \leq \alpha_0^{-2}$. \square

3.4 A conservative explicit estimate of ρ_{\max}

The strong bounds depend on ρ_{\max} . A convenient conservative estimate can be obtained from a linearized hypoelliptic Gaussian upper bound (see also related density estimates for linear diffusions).

Assumption 3.9 (Effective diffusion in the current). For each neuron (ℓ, j) , the current can be modeled (or approximated, e.g. by a diffusion approximation of many small independent synaptic inputs) as

$$dI_{\ell,j}(t) = -\frac{1}{\tau_c}(I_{\ell,j}(t) - \mu_{\ell,j}(t)) dt + \frac{\sigma_{\text{eff},\ell,j}(t)}{\tau_c} dB_{\ell,j}(t), \quad (19)$$

with $\sigma_{\text{eff},\ell,j}(t) \geq \sigma_{\min} > 0$ and bounded $\mu_{\ell,j}(t)$. For feedforward inputs, a standard Poisson \rightarrow Gaussian approximation yields

$$\sigma_{\text{eff},\ell,j}^2(t) \approx (\sigma_{\ell,j}^{\text{ext}})^2 + \kappa \tau_c^2 \sum_{i=1}^{n_{\ell-1}} (W_{ji}^{\ell-1,\ell})^2 r_{\ell-1,i}(t), \quad (20)$$

where $r_{\ell-1,i}(t)$ are presynaptic firing rates and κ is the approximation constant.

Lemma 3.10 (Explicit stationary Gaussian supremum bound). *Assume coefficients are time-independent and (19) holds with constant $\sigma_{\text{eff}} > 0$. Consider the corresponding linear (v, I) system without threshold/reset:*

$$dv = \left(-\frac{1}{\tau_v}(v - V_r) + I\right) dt, \quad dI = -\frac{1}{\tau_c}(I - \mu) dt + \frac{\sigma_{\text{eff}}}{\tau_c} dB.$$

Its stationary joint density is Gaussian with

$$\sup_{(v,I) \in \mathbb{R}^2} \rho_{\text{lin}}(v, I, \infty) = \frac{\sqrt{\tau_c}(\tau_c + \tau_v)}{\pi \sigma_{\text{eff}}^2 \tau_v^{3/2}}. \quad (21)$$

Consequently, for the reset system one may take the conservative explicit bound

$$\rho_{\max,\ell,j}(T, \alpha_0) \leq \frac{\sqrt{\tau_c}(\tau_c + \tau_v)}{\pi \sigma_{\text{eff},\ell,j}^2 \tau_v^{3/2}}. \quad (22)$$

Proof. A direct Lyapunov-equation computation gives the stationary covariance of the linear system:

$$\text{Var}(I) = \frac{\sigma_{\text{eff}}^2}{2\tau_c}, \quad \text{Cov}(v, I) = \frac{\sigma_{\text{eff}}^2 \tau_v}{2(\tau_c + \tau_v)}, \quad \text{Var}(v) = \frac{\sigma_{\text{eff}}^2 \tau_v^2}{2(\tau_c + \tau_v)}.$$

Thus $\det C_\infty = \frac{\sigma_{\text{eff}}^4 \tau_v^3}{4\tau_c(\tau_c + \tau_v)^2}$ and the maximum of a 2D Gaussian density is $(2\pi\sqrt{\det C_\infty})^{-1}$, yielding (21). For the reset system, the density can be represented as a convex mixture (renewal decomposition) of hypoelliptic transition densities from reset states; taking pointwise suprema yields the conservative bound (22). \square

Lemma 3.11 (Conservative explicit bound for the voltage strip density). *Assume coefficients are time-independent and Assumption 3.9 holds with constant $\sigma_{\text{eff}} > 0$. For the corresponding linear (v, I) system without threshold/reset (as in Lemma 3.10), the stationary voltage marginal is Gaussian with variance*

$$\text{Var}(v) = \frac{\sigma_{\text{eff}}^2 \tau_v^2}{2(\tau_c + \tau_v)}.$$

Hence

$$\sup_{v \in \mathbb{R}} \varrho_{\text{lin}}^V(v, \infty) = \frac{1}{\sqrt{2\pi} \text{Var}(v)} = \frac{\sqrt{\tau_c + \tau_v}}{\sqrt{\pi} \sigma_{\text{eff}} \tau_v}.$$

Consequently, for the reset system one may take the conservative explicit bound

$$\rho_{\text{max}, \ell, j}^V(T) \leq \frac{\sqrt{\tau_c + \tau_v}}{\sqrt{\pi} \sigma_{\text{eff}, \ell, j} \tau_v}. \quad (23)$$

Proof. The linear-system variance is stated in Lemma 3.10; the displayed supremum is the maximum of a one-dimensional Gaussian density. For the reset system, represent the law at time t as a convex mixture of transition laws from post-reset states; taking pointwise suprema yields the conservative bound (23). \square

Remark 3.12 (OU surrogate vs. reset density near threshold). Lemmas 3.10–3.11 compute stationary Gaussian suprema for the full-space linear OU diffusion (with no threshold/reset). The true hybrid process has a density $\rho(v, I, t)$ on the subthreshold domain $\{v < V_{\text{th}}\}$ that solves a kinetic Fokker–Planck equation with an absorbing boundary at $v = V_{\text{th}}$ and a reinjection source at $v = V_{\text{r}}$ whose intensity is the threshold flux. Formally one can write a renewal representation

$$\rho(\cdot, t) = P_t^0 \rho(\cdot, 0) + \int_0^t P_{t-s}^0 \mathcal{R}J(s) ds,$$

where P_t^0 is the killed semigroup, $J(s)$ is the boundary flux, and \mathcal{R} applies the reset map. In feedforward networks, and in recurrent networks in asynchronous regimes where $\mu(t)$ is effectively exogenous to $B(t)$ and the flux $J(s)$ is not concentrated in short bursts, the boundary-strip densities defining ρ_{max} and ρ_{max}^V are typically of the same order as the OU proxies (22)–(23). However, in synchronized regimes the reinjection term can create sharp boundary layers near V_{th} and these proxies can fail (see also Remark 6.8).

Remark 3.13 (How Lemma 3.11 enters later bounds). The abstract density bound (57) (and its weak-error analogue (57)) is stated as an assumption because it is a property of the *reset* dynamics. Lemma 3.11 provides a conservative *explicit* sufficient bound for the corresponding strip constant $\rho_{\text{max}, \ell, j}^V(T)$ under a time-homogeneous OU surrogate for $I_{\ell, j}$. We will invoke $\rho_{\text{max}, \ell, j}^V(T)$ later whenever we need an explicit bound on the probability that the voltage lies in a thin strip below threshold (e.g. in the weak error analysis of Section 4, and in conservative estimates in regimes with frequent near-threshold visits).

Remark 3.14 (Dependence on W through effective noise). Assumption 3.9 makes the dependence of ρ_{max} on feedforward weights explicit: larger $\sum_i (W_{ji}^{\ell-1, \ell})^2 r_{\ell-1, i}$ increases effective noise and thus decreases ρ_{max} , making near-tangential spikes rarer.

3.5 Spike-count mismatch bad set (sharp)

The stepwise spike decision mismatch $\{S_m \neq \hat{S}_m\}$ is too pessimistic for strong error: a spike that is advanced/delayed by a small amount produces a short time interval on which spike counts differ, but the counts typically *catch up* immediately and the spike trains can still be paired by index. For the pruning argument we therefore declare a trajectory bad only if the spike *counts at the horizon* differ.

Count mismatch. For each neuron (ℓ, j) define the spike-count mismatch event

$$B_{\ell, j}^{\text{mis}}(h, T) := \{N_{\ell, j}^h(T) \neq N_{\ell, j}(T)\},$$

as already introduced in (11). This bad set is independent of the tangency cutoff α .

A deterministic reduction to boundary and burst events. Fix a tolerance $\delta > 0$ and define, whenever both k th spikes exist, $\varepsilon_{\ell,j}^k := \hat{s}_{\ell,j}^k - s_{\ell,j}^k$; set $|\varepsilon_{\ell,j}^k| := \infty$ otherwise. Introduce the auxiliary events

$$B_{\ell,j}^{\partial}(\delta, T) := \{N_{\ell,j}(T + \delta) - N_{\ell,j}(T - \delta) \geq 1\}, \quad (24)$$

$$B_{\ell,j}^{(2)}(\delta, T) := \{\exists k : s_{\ell,j}^k \leq T + \delta \text{ and } s_{\ell,j}^{k+1} - s_{\ell,j}^k \leq 2\delta\}, \quad (25)$$

$$B_{\ell,j}^{\text{err}}(h, \delta, T) := \left\{ \max_{k: s_{\ell,j}^k \leq T + \delta} |\varepsilon_{\ell,j}^k| > \delta \right\}. \quad (26)$$

Lemma 3.15 (Count mismatch decomposition). *For any $\delta > 0$,*

$$B_{\ell,j}^{\text{mis}}(h, T) \subseteq B_{\ell,j}^{\partial}(\delta, T) \cup B_{\ell,j}^{(2)}(\delta, T) \cup B_{\ell,j}^{\text{err}}(h, \delta, T).$$

Proof. Assume $B_{\ell,j}^{\partial}(\delta, T)^c \cap B_{\ell,j}^{(2)}(\delta, T)^c \cap B_{\ell,j}^{\text{err}}(h, \delta, T)^c$. Then there is no exact spike in $(T - \delta, T + \delta)$, and all exact interspike gaps up to $T + \delta$ exceed 2δ . Moreover, for every exact spike time $s_{\ell,j}^k \leq T + \delta$, the corresponding numerical spike time $\hat{s}_{\ell,j}^k$ exists and satisfies $|\hat{s}_{\ell,j}^k - s_{\ell,j}^k| \leq \delta$. The separation $s_{\ell,j}^{k+1} - s_{\ell,j}^k > 2\delta$ implies that the intervals $[s_{\ell,j}^k - \delta, s_{\ell,j}^k + \delta]$ are disjoint and preserve ordering, so $\hat{s}_{\ell,j}^k < \hat{s}_{\ell,j}^{k+1}$. Since no spike lies within δ of T , we have $s_{\ell,j}^k \leq T$ if and only if $\hat{s}_{\ell,j}^k \leq T$ for every k . Hence $N_{\ell,j}^h(T) = N_{\ell,j}(T)$, contradicting $B_{\ell,j}^{\text{mis}}(h, T)$. \square

Probability bound and scaling in T and h . To turn Lemma 3.15 into a sharp probability estimate we use two spike-train regularity controls.

(M1) **Local rate bound near T .** There exists $r_{\ell,j}^{\max}(T) < \infty$ such that for all $\delta \in (0, 1]$,

$$\mathbb{E}[N_{\ell,j}(T + \delta) - N_{\ell,j}(T - \delta)] \leq 2r_{\ell,j}^{\max}(T)\delta. \quad (27)$$

(M2) **No-burst (pair) bound.** There exists $R_{\ell,j}^{(2)}(T) < \infty$ such that for all $\eta \in (0, 1]$,

$$\mathbb{E}\left[\sum_{k \neq m: s_{\ell,j}^k, s_{\ell,j}^m \leq T + 1} \mathbb{1}_{\{|s_{\ell,j}^k - s_{\ell,j}^m| \leq \eta\}} \right] \leq R_{\ell,j}^{(2)}(T)\eta^2. \quad (28)$$

The bound (27) is controlled by the firing rate near the horizon, while (28) controls bursty regimes in which two spikes may occur within a very short window.

In addition, we will use that spike-time errors have Gaussian-type concentration at scale \sqrt{h} . We record this as an assumption tailored to the current-driven LIF setting (where all driving noises are Gaussian): there exist constants $C_{\text{sg}}, c_{\text{sg}} > 0$ such that for all $\delta \in (0, 1]$,

$$\sup_{k \geq 1} \mathbb{P}(|\varepsilon_{\ell,j}^k| > \delta, s_{\ell,j}^k \leq T + 1) \leq C_{\text{sg}} \exp\left(-c_{\text{sg}} \frac{\delta^2}{h}\right). \quad (29)$$

Lemma 3.16 (Spike-count mismatch probability). *Assume (27), (28), and (29). Then for any $\delta \in (0, 1]$,*

$$\mathbb{P}(B_{\ell,j}^{\text{mis}}(h, T)) \leq 2r_{\ell,j}^{\max}(T)\delta + 4R_{\ell,j}^{(2)}(T)\delta^2 + C_{\ell,j}^{\text{err}}(T) \exp\left(-c_{\text{sg}} \frac{\delta^2}{h}\right), \quad (30)$$

where $C_{\ell,j}^{\text{err}}(T) := C_{\text{sg}}\mathbb{E}[N_{\ell,j}(T + 1)]$. In particular, choosing $\delta = \delta_h := \kappa\sqrt{h \log(1/h)}$ yields

$$\mathbb{P}(B_{\ell,j}^{\text{mis}}(h, T)) \lesssim r_{\ell,j}^{\max}(T) \sqrt{h \log(1/h)} + R_{\ell,j}^{(2)}(T) h \log(1/h) + C_{\ell,j}^{\text{err}}(T) h^{c_0}, \quad c_0 := c_{\text{sg}}\kappa^2. \quad (31)$$

Proof. By Lemma 3.15 and the union bound,

$$\mathbb{P}(B_{\ell,j}^{\text{mis}}(h, T)) \leq \mathbb{P}(B_{\ell,j}^{\partial}(\delta, T)) + \mathbb{P}(B_{\ell,j}^{(2)}(\delta, T)) + \mathbb{P}(B_{\ell,j}^{\text{err}}(h, \delta, T)).$$

For the boundary term, Markov's inequality and (27) give

$$\mathbb{P}(B_{\ell,j}^{\partial}(\delta, T)) \leq \mathbb{E}[N_{\ell,j}(T + \delta) - N_{\ell,j}(T - \delta)] \leq 2 r_{\ell,j}^{\text{max}}(T) \delta.$$

For the burst term, note that $B_{\ell,j}^{(2)}(\delta, T)$ implies the existence of a pair of distinct spikes within distance 2δ before time $T + 1$ (since $\delta \leq 1$). Markov's inequality and (28) yield

$$\mathbb{P}(B_{\ell,j}^{(2)}(\delta, T)) \leq \mathbb{E} \left[\sum_{k \neq m: s_{\ell,j}^k, s_{\ell,j}^m \leq T+1} \mathbb{1}_{\{|s_{\ell,j}^k - s_{\ell,j}^m| \leq 2\delta\}} \right] \leq 4 R_{\ell,j}^{(2)}(T) \delta^2.$$

Finally, by the union bound and (29),

$$\mathbb{P}(B_{\ell,j}^{\text{err}}(h, \delta, T)) \leq \mathbb{E} \left[\sum_{k: s_{\ell,j}^k \leq T+1} \mathbb{1}_{\{|\varepsilon_{\ell,j}^k| > \delta\}} \right] \leq \mathbb{E}[N_{\ell,j}(T + 1)] C_{\text{sg}} \exp\left(-c_{\text{sg}} \frac{\delta^2}{h}\right),$$

which gives (30). Choosing $\delta = \delta_h$ gives (31) since $\exp(-c_{\text{sg}} \delta_h^2/h) = \exp(-c_{\text{sg}} \kappa^2 \log(1/h)) = h^{c_{\text{sg}} \kappa^2}$. \square

Remark 3.17 (Why the h^{c_0} term can be neglected). In (31) the exponent $c_0 = c_{\text{sg}} \kappa^2$ comes from the Gaussian-type concentration (29) and the choice $\delta_h = \kappa \sqrt{h \log(1/h)}$. Since $\kappa > 0$ is free, we may choose it so that $c_0 > 1/2$. For fixed T (hence $\mathbb{E}[N_{\ell,j}(T + 1)] = O(T)$), this implies $h^{c_0} = o(h^{1/2})$ as $h \rightarrow 0$, and therefore the last term in (31) is negligible compared with the leading boundary contribution $O(\sqrt{h \log(1/h)})$.

Remark 3.18 (Dependence on L , T , and W of the mismatch term). Lemma 3.16 yields a *spike-count* mismatch probability controlled by three mechanisms: (i) a *boundary-at- T* contribution of order $r_{\ell,j}^{\text{max}}(T) \sqrt{h \log(1/h)}$, (ii) an *interior burst* contribution of order $R_{\ell,j}^{(2)}(T) h \log(1/h)$, and (iii) an exponentially small-in- δ^2/h remainder (cf. Remark 3.17). Importantly, this term is independent of the tangency cutoff α and therefore does not interact with the α -balancing that governs the good-set/tangency contributions.

In the strong pruning bound (43), mismatch enters only through $\mathbb{P}(B_{\ell,j}^{\text{mis}}(h, T))$. Thus mismatch does *not* propagate with depth through the spike-time recursion; depth deterioration of the strong rate is driven by the good-set spike-time amplification, while mismatch is controlled by firing activity near the horizon and by burst statistics (captured by r^{max} and $R^{(2)}$).

3.6 Propagation of spike-time errors across feedforward layers

We now quantify how presynaptic STE induces postsynaptic current/voltage perturbations. The key technical point is the *jump misalignment window*: pointwise current differences are not Lipschitz in time shift, but their time integrals are.

3.6.1 Synaptic kernel and the misalignment window

For $\ell \geq 2$, the contribution of a presynaptic spike at time s to the postsynaptic current has kernel

$$K(t; s) := \exp\left(-\frac{t-s}{\tau_c}\right) \mathbb{1}_{\{t \geq s\}}.$$

If the same spike is shifted to $\hat{s} = s + \varepsilon$, then $K(\cdot; s)$ and $K(\cdot; \hat{s})$ differ by $O(1)$ on the misalignment window (s, \hat{s}) , so L^∞ is not Lipschitz. However:

Lemma 3.19 (Misalignment window: L^∞ is not Lipschitz, but L^1 is). *Let $K(t; s) = e^{-(t-s)/\tau_c} \mathbb{1}_{\{t \geq s\}}$ and $\hat{s} = s + \varepsilon$. Then*

$$\sup_{t \in [0, T]} |K(t; s) - K(t; \hat{s})| = \mathbb{1}_{\{\varepsilon \neq 0\}}, \quad (32)$$

$$\int_0^T |K(t; s) - K(t; \hat{s})| dt = 2\tau_c(1 - e^{-|\varepsilon|/\tau_c}) \leq 2|\varepsilon|. \quad (33)$$

Proof. Direct computation, splitting at the window $(s, s + \varepsilon)$ and using $1 - e^{-x/\tau_c} \leq x/\tau_c$. \square

3.6.2 L_t^1 current perturbation induced by presynaptic STE

Define the row- ℓ^1 matrix norm

$$\|W^{\ell-1, \ell}\|_\infty := \max_{1 \leq j \leq n_\ell} \sum_{i=1}^{n_{\ell-1}} |W_{ji}^{\ell-1, \ell}|.$$

Let $\Delta_\ell(T)$ denote the layerwise RMS STE magnitude on the good event:

$$\Delta_\ell(T) := \max_{1 \leq j \leq n_\ell} \max_{k: s_{\ell, j}^k \leq T} \mathbb{E} \left[\left| \varepsilon_{\ell, j}^k \right|^2 \mathbb{1}_{G_\ell(h, T; \alpha)} \right]^{1/2}.$$

To quantify spike load, let

$$\Lambda_\ell(T) := \max_{1 \leq i \leq n_\ell} \#\{k : s_{\ell, i}^k \leq T\}, \quad (34)$$

interpreted as a deterministic bound on the good event (e.g. $\Lambda_\ell(T) \leq r_\ell^{\max} T$ if rates are bounded on G_L).

Lemma 3.20 (Postsynaptic current sensitivity in L_t^1). *Fix $\ell \geq 2$ and neuron (ℓ, j) . On the good event $G_\ell(h, T; \alpha)$ (spike trains in layers $\leq \ell$ are matched),*

$$\int_0^T |I_{\ell, j}(t) - I_{\ell, j}^h(t)| dt \leq T C_{\ell, j}^{I, \text{loc}}(T) h^{1/2} + 2 \sum_{i=1}^{n_{\ell-1}} |W_{ji}^{\ell-1, \ell}| \sum_{k: s_{\ell-1, i}^k \leq T} |\varepsilon_{\ell-1, i}^k|. \quad (35)$$

Consequently,

$$\mathbb{E} \left[\left(\int_0^T |I_{\ell, j}(t) - I_{\ell, j}^h(t)| dt \right)^2 \mathbb{1}_{G_\ell} \right]^{1/2} \leq T C_{\ell, j}^{I, \text{loc}}(T) h^{1/2} + 2 \|W^{\ell-1, \ell}\|_\infty \Lambda_{\ell-1}(T) \Delta_{\ell-1}(T). \quad (36)$$

Proof. Decompose $I_{\ell, j}$ into a local OU-driven part and a feedforward jump-driven part. The local part has EM strong order 1/2 in L^2 , yielding the first term. For the feedforward part, on G_ℓ spikes are matched; subtract kernel sums and apply the L^1 shift bound (33) to each spike to get the second term. The RMS bound follows from $\sum_k |\varepsilon^k| \leq \Lambda \max_k |\varepsilon^k|$ on G_ℓ . \square

3.6.3 Voltage perturbation is Lipschitz in L_t^1 current perturbation

Lemma 3.21 (Voltage L_t^1 stability). *On an interval without resets, if v and \tilde{v} solve $\dot{v} = -\tau_v^{-1}(v - V_r) + I(t)$ and $\dot{\tilde{v}} = -\tau_v^{-1}(\tilde{v} - V_r) + \tilde{I}(t)$ with the same initial condition, then*

$$\sup_{t \in [t_0, t_1]} |v(t) - \tilde{v}(t)| \leq \int_{t_0}^{t_1} |I(s) - \tilde{I}(s)| ds. \quad (37)$$

Proof. Subtract equations to get $\dot{e} = -\tau_v^{-1}e + (I - \tilde{I})$ and apply variation of constants. \square

Remark 3.22 (Where the misalignment window is “paid for”). Lemma 3.19 shows $|I - I^h|$ can be $O(1)$ pointwise on a window of length $|\varepsilon|$, but Lemma 3.21 integrates that window, yielding an $O(|\varepsilon|)$ contribution to voltage error. This is the correct notion of Lipschitz continuity for propagation of STE.

3.6.4 Layerwise STE recursion (explicit constants)

Define $\tau_* := \min\{\tau_v, \tau_c\}$. An explicit local constant capturing subthreshold EM error and linear stability may be taken as

$$C_\ell^{\text{loc}}(T) := c_0 (1 + T) \exp\left(\frac{T}{\tau_*}\right) \max_{1 \leq j \leq n_\ell} \left(1 + |v_{\ell,j}(0)| + |I_{\ell,j}(0)| + \|b_{\ell,j}\|_\infty + \sigma_{\ell,j}\right), \quad (38)$$

with a universal $c_0 > 0$.

Assumption 3.23 (Conditional local strong error near spikes). For each layer ℓ and each neuron (ℓ, j) , the local subthreshold discretization error does not concentrate on small crossing speeds: for every spike index k with $s_{\ell,j}^k \leq T$,

$$\mathbb{E} \left[\sup_{t \in [s_{\ell,j}^k - h, s_{\ell,j}^k + h]} \left| v_{\ell,j}(t) - v_{\ell,j}^h(t) \right|^2 \mid A_{\ell,j}^k \right] \leq (C_\ell^{\text{loc}}(T))^2 h. \quad (39)$$

Theorem 3.24 (STE recursion across layers). Fix $T > 0$ and truncation thresholds $\alpha_1, \dots, \alpha_L \in (0, \alpha_0]$. For each layer ℓ , define the truncated inverse-moment factor

$$\mathbf{m}_\ell(T; \alpha_\ell) := \max_{1 \leq j \leq n_\ell} \left(\frac{1}{\alpha_0^2} + T \rho_{\max, \ell, j}(T, \alpha_0) \log \frac{\alpha_0}{\alpha_\ell} \right)^{1/2}. \quad (40)$$

Assume the conditional non-concentration bound (39) holds at every layer (with possibly layer-dependent constants absorbed into $C_\ell^{\text{loc}}(T)$). Then, on the good event $G_\ell(h, T; \alpha)$, for $\ell \geq 2$,

$$\Delta_\ell(T) \leq \mathbf{m}_\ell(T; \alpha_\ell) \left(C_\ell^{\text{loc}}(T) h^{1/2} + 2 \|W^{\ell-1, \ell}\|_\infty \Lambda_{\ell-1}(T) \Delta_{\ell-1}(T) \right). \quad (41)$$

For $\ell = 1$, $\Delta_1(T) \leq \mathbf{m}_1(T; \alpha_1) C_1^{\text{loc}}(T) h^{1/2}$ on G_1 .

Proof. The proof follows the same steps as in the conservative bound, except that we retain the random crossing speed $A_{\ell,j}^k$ in Lemma 3.4 and use the log-truncated inverse moment (Lemma 3.8) instead of the worst-case bound $A_{\ell,j}^k \geq \alpha_\ell$.

For $\ell \geq 2$, Lemma 3.20 yields an L^1 bound on the synaptic input error in terms of the upstream spike-time errors, and Lemma 3.21 converts this to a voltage error bound on the crossing interval. Combining with Lemma 3.4 gives, for each spike $s_{\ell,j}^k \leq T$ on $G_\ell(h, T; \alpha)$,

$$\left| \varepsilon_{\ell,j}^k \right| \leq h + \frac{1}{A_{\ell,j}^k} \left(C_\ell^{\text{loc}}(T) h^{1/2} + 2 \|W^{\ell-1, \ell}\|_\infty \Lambda_{\ell-1}(T) \Delta_{\ell-1}(T) \right).$$

Squaring, taking expectations, and using the conditional bound (39) together with Lemma 3.8 (layer ℓ) yields the factor $\mathbf{m}_\ell(T; \alpha_\ell)^2$. The additive h term from Lemma 3.4 contributes only $O(h^2)$ to $\Delta_\ell(T)^2$ and is absorbed into constants. Taking the maximum over spikes and neurons gives (41). The case $\ell = 1$ is identical but without the synaptic input term. \square

3.7 Network strong error bound via pruning

3.7.1 Network good/bad events

Let $G_L(h, T; \alpha)$ be the event that, for all layers $\ell \leq L$ and all neurons j :

(G1) **Spike-count matching at the horizon:** $N_{\ell,j}^h(T) = N_{\ell,j}(T)$ (equivalently, the spike trains up to time T can be paired by index);

(G2) **Uniform transversality:** all exact spikes up to time T satisfy $A_{\ell,j}^k \geq \alpha_\ell$.

Let $B_L(h, T; \alpha) := G_L(h, T; \alpha)^c$.

3.7.2 Pruning decomposition

Let $X_L(T)$ be any bounded functional of the network output at time T (e.g. the layer- L state). Then

$$\mathbb{E}\left[\left\|X_L^h(T) - X_L(T)\right\|^2\right] \leq \mathbb{E}\left[\left\|X_L^h(T) - X_L(T)\right\|^2 \mathbb{1}_{G_L(h,T;\alpha)}\right] + C_{\max}^2 \mathbb{P}(B_L(h,T;\alpha)), \quad (42)$$

where C_{\max} bounds $\|X_L^h(T) - X_L(T)\|$ pointwise.

3.7.3 Bounding the bad probability (explicit α and T dependence)

Proposition 3.25 (Tangency and mismatch contributions to the bad probability). *Assume (14) holds. Then*

$$\mathbb{P}(B_L(h,T;\alpha)) \leq \sum_{\ell=1}^L \sum_{j=1}^{n_\ell} \mathbb{P}(B_{\ell,j}^{\text{mis}}(h,T)) + \frac{T}{2} \sum_{\ell=1}^L \sum_{j=1}^{n_\ell} \rho_{\max,\ell,j}(T, \alpha_0) \alpha_\ell^2. \quad (43)$$

Proof. Union bound over layers/neurons, Lemma 3.16, and Lemma 3.7. \square

3.7.4 Iterating the STE recursion

Define the layer gains

$$G_\ell^{\text{loc}}(T) := \frac{C_\ell^{\text{loc}}(T)}{\alpha_\ell}, \quad G_\ell^{\text{net}}(T) := \frac{2}{\alpha_\ell} \|W^{\ell-1,\ell}\|_\infty \Lambda_{\ell-1}(T) \quad (\ell \geq 2).$$

Proposition 3.26 (Iterating the recursion). *Iterating (41) yields the explicit bound*

$$\Delta_L(T) \leq h^{1/2} \sum_{m=1}^L \left(C_m^{\text{loc}}(T) \mathbf{m}_m(T; \alpha_m) \prod_{r=m+1}^L \left(2 \|W^{r-1,r}\|_\infty \Lambda_{r-1}(T) \mathbf{m}_r(T; \alpha_r) \right) \right), \quad (44)$$

with the usual convention that an empty product equals 1. Under the simplifying uniform assumptions

$$n_\ell \equiv n, \quad \|W^{\ell-1,\ell}\|_\infty \leq \mathcal{W}, \quad C_\ell^{\text{loc}}(T) \leq C^{\text{loc}}(T), \quad \mathbf{m}_\ell(T; \alpha_\ell) \leq \mathbf{m}(T; \alpha), \quad (45)$$

one obtains the geometric-series bound

$$\Delta_L(T) \leq C^{\text{loc}}(T) h^{1/2} \mathbf{m}(T; \alpha) \sum_{q=0}^{L-1} \left(2\mathcal{W} \Lambda(T) \mathbf{m}(T; \alpha) \right)^q. \quad (46)$$

In particular, when $2\mathcal{W} \Lambda(T) \mathbf{m}(T; \alpha) \gtrsim 1$ (true when $\alpha \rightarrow 0$), the leading behavior is $\Delta_L(T) \lesssim C^{\text{loc}}(T) h^{1/2} (2\mathcal{W} \Lambda(T))^{L-1} \mathbf{m}(T; \alpha)^L$, so the depth dependence enters through a factor $\mathbf{m}(T; \alpha)^L \sim (T \log(\alpha_0/\alpha))^{L/2}$ in RMS.

Proof. The identity (44) is obtained by repeated substitution of (41). The simplified bound (46) follows from (45) and bounding each product by $(2\mathcal{W} \Lambda(T) \mathbf{m}(T; \alpha))^q$. \square

3.7.5 A strong MSE bound explicit in T , L , and weights

Assume that on G_L the output functional is Lipschitz in the layer- L spike-time metric: there exists Lip_X such that $\|X_L^h(T) - X_L(T)\| \leq \text{Lip}_X \Delta_L(T)$ on G_L . Then combining (42)–(43) with Proposition 3.26 yields

$$\mathbb{E} \left[\left\| X_L^h(T) - X_L(T) \right\|^2 \right] \leq \text{Lip}_X^2 \Delta_L(T)^2 + C_{\max}^2 \left(\sum_{\ell=1}^L \sum_{j=1}^{n_\ell} \mathbb{P}(B_{\ell,j}^{\text{mis}}(h, T)) + \frac{T}{2} \sum_{\ell=1}^L \sum_{j=1}^{n_\ell} \rho_{\max, \ell, j}(T, \alpha_0) \alpha_\ell^2 \right), \quad (47)$$

where $\Delta_L(T)$ is given by (44) and all constants are explicit.

We will soon reveal that, when balancing the choices of α , the squared strong error $\mathbb{E} \left[\left\| X_L^h(T) - X_L(T) \right\|^2 \right]$ is dominated by the mismatch error of order $O(Th^{1/2})$. When the boundary mismatch is not taking place, $\mathbb{E} \left[\left\| X_L^h(T) - X_L(T) \right\|^2 \right]$ is of order $O(h)$ multiplied by polylogarithmic.

3.7.6 Interpretation: depth and time growth in the pruning bound

To make the scaling transparent, assume for simplicity that the network is reasonably homogeneous in the sense of (45). Abbreviate the representative (layer-wise) inverse-moment factor by

$$\mathbf{m}(T; \alpha) := \left(\frac{1}{\alpha_0^2} + T \rho_{\max}(T, \alpha_0) \log \frac{\alpha_0}{\alpha} \right)^{1/2}, \quad (48)$$

where $\rho_{\max}(T, \alpha_0) := \max_{\ell, j} \rho_{\max, \ell, j}(T, \alpha_0)$. Then Proposition 3.26 shows that the good-set RMS spike-time error envelope at depth L obeys

$$\Delta_L(T) \lesssim C^{\text{loc}}(T) h^{1/2} \mathbf{m}(T; \alpha) \sum_{q=0}^{L-1} \left(2\mathcal{W} \Lambda(T) \mathbf{m}(T; \alpha) \right)^q,$$

so that each layer contributes *one* factor of $\mathbf{m}(T; \alpha)$, regardless of whether the numerator originates from a local discretization error or from propagated upstream errors. In particular, in the regime $2\mathcal{W} \Lambda(T) \mathbf{m}(T; \alpha) \gtrsim 1$,

$$\Delta_L(T) \lesssim C^{\text{loc}}(T) h^{1/2} (2\mathcal{W} \Lambda(T))^{L-1} \mathbf{m}(T; \alpha)^L. \quad (49)$$

When the logarithmic part dominates in (48) (i.e. $T \rho_{\max}(T, \alpha_0) \log(\alpha_0/\alpha) \gg \alpha_0^{-2}$), one has $\mathbf{m}(T; \alpha)^L \asymp (T \rho_{\max}(T, \alpha_0))^{L/2} (\log(\alpha_0/\alpha))^{L/2}$, so the *cutoff dependence* is only through $\log(\alpha_0/\alpha)$. This is the source of the $\log(1/\alpha)^{L/2}$ depth factor in the good-set strong error, while the remaining T - and weight-dependence is carried by $\rho_{\max}(T, \alpha_0)$, $\Lambda(T)$ and \mathcal{W} .

A consistent schematic pruning trade-off (ignoring mismatch). Write $b(T) := T \rho_{\max}(T, \alpha_0)$ and $c(T) = 2\mathcal{W} \Lambda(T)$. Up to T - and L -dependent prefactors coming from weight norms and spike-train Lipschitz constants, the pruning bound (47) has the schematic form

$$\text{MSE}(\alpha) \lesssim h \cdot \left[C^{\text{loc}}(T) c^{L-1}(T) \right]^2 \left(\alpha_0^{-2} + b(T) \log(\alpha_0/\alpha) \right)^L + b(T) \alpha^2. \quad (50)$$

(The first term reflects the good-set STE estimate with $\mathbf{m}(T; \alpha)^{2L}$, while the second is the tangency mass $O(T \rho_{\max} \alpha^2)$.) We note that $b(T)$, $c(T)$, and $C^{\text{loc}}(T)$ are all $O(T)$.

Since the good-set term depends on α only through $-\log \alpha$, while the tangency-bad probability is quadratic in α , the optimizer is substantially less sensitive to the cutoff than in the worst-case $1/\alpha$ analysis. Differentiating the right-hand side of (50) yields the implicit balance

$$2\alpha^2 \asymp h L \left[C^{\text{loc}}(T) c^{L-1}(T) \right]^2 \left(\alpha_0^{-2} + b(T) \log(\alpha_0/\alpha) \right)^{L-1}.$$

We record the corresponding cutoff selection rule as

$$\alpha(h, T)^2 \asymp h T^{2L} \left(\alpha_0^{-2} + b(T) \log \frac{\alpha_0}{\alpha(h, T)} \right)^{L-1}, \quad 0 < \alpha(h, T) \leq \alpha_0, \quad (51)$$

where the constant in \asymp absorbs the factor L and factors of $c(T), C^{\text{loc}}(T)$.

In the dominant-log regime, a first iteration gives the explicit approximation $\alpha(h, T) \approx \sqrt{h} T^L b(T)^{\frac{L-1}{2}} (\log(\alpha_0/\sqrt{h}))^{\frac{L-1}{2}}$ (clipped at α_0). With such choices, the good-set contribution scales like $\text{MSE}_{\text{good}} \lesssim h T^{2L} (\alpha_0^{-2} + b(T) \log(\alpha_0/\alpha))^L$ and hence $\text{RMS}_{\text{good}} \lesssim h^{1/2} T^L (\alpha_0^{-2} + b(T) \log(\alpha_0/\alpha))^{L/2}$.

Remark 3.27 (A suboptimal α). There is a lazy way to take $\alpha^2 \asymp h$, leading to a clearer way of the order- $\frac{1}{2}$ -plus-polylogarithmic nature of $\text{MSE}_{\text{good}} = O(h \cdot (\frac{1}{2} T^3 \log h)^L)$

Remark 3.28 (From fixed- T pruning bounds to long-time behavior). The log-truncated inverse-moment estimate changes the nature of the α -trade-off. On the one hand, the tangency-bad probability remains quadratic in α (Lemma 3.7). On the other hand, the good-set strong error depends on α only through $\log(\alpha_0/\alpha)$ (Lemma 3.8), reflecting the integrable a^{-1} singularity of the flux measure near $A = 0$ under the boundary density bound. Accordingly, the cutoff is governed by the implicit relation (51) rather than an algebraic power of h .

Two caveats are important.

- First, both $\rho_{\max}(T, \alpha_0)$ and the spike-train factors $\Lambda(T)$ (and, in recurrent settings, the effective event depth) typically depend on T and on synaptic weights, so one should not extrapolate fixed- T asymptotics to $T \rightarrow \infty$ without additional control of these quantities.
- Second, for schemes that detect spikes only through grid endpoint tests, spike-count mismatches at the observation time can dominate the overall strong rate for discontinuous observables. By Lemma 3.16, the spike-count mismatch probability is controlled by a boundary-at- T term $O(r^{\max}(T) \sqrt{h \log(1/h)})$ and a burst term $O(R^{(2)}(T) h \log(1/h))$ (up to a negligible h^{c_0} remainder). This contribution is independent of the tangency cutoff α and therefore does not affect the α -balancing that governs the good-set/tangency terms.

3.8 When depth does not deteriorate the strong exponent

The depth dependence in the pruning bounds is driven by two mechanisms: (i) in fluctuation-driven layers, crossings can be nearly tangential ($A = I - I_{\text{th}} \approx 0$) and force $\alpha \rightarrow 0$ as $h \rightarrow 0$; (ii) if independent current noise enters *each* layer, new small-speed events are created layerwise and the STE recursion accumulates *one* inverse-moment factor $\mathbf{m}_\ell(T; \alpha_\ell)$ per noisy layer (equivalently, one $\sqrt{\log(\alpha_0/\alpha_\ell)}$ factor in the homogeneous regime).

A single structural condition removes mechanism (ii): no intrinsic current noise is injected in layers $\ell \geq 2$. Then all downstream randomness is transported only through the spike times arriving from upstream, and the good-set strong rate is inherited from the first layer (up to deterministic downstream stability factors).

3.8.1 No intrinsic noise downstream

Assumption 3.29 (No intrinsic current noise in layers $\ell \geq 2$). For every neuron (ℓ, j) with $\ell \geq 2$ we have $\sigma_{\ell, j} = 0$ in (2).

Assumption 3.30 (Downstream transversality margin). For each $\ell \in \{2, \dots, L\}$ there exists $\alpha_\ell^{\text{MD}} > 0$ such that for every neuron (ℓ, j) and every spike time $s_{\ell, j}^k \leq T$,

$$A_{\ell, j}^k = I_{\ell, j}(s_{\ell, j}^k -) - I_{\text{th}} \geq \alpha_\ell^{\text{MD}}. \quad (52)$$

Theorem 3.31 (No downstream noise: the strong h -exponent is inherited from layer 1). *Assume Assumptions 3.29 and 3.30. Fix $T > 0$. Choose $\alpha_\ell = \alpha_\ell^{\text{MD}}$ for $\ell \geq 2$ and choose $\alpha_1 \in (0, \alpha_0]$ (possibly depending on h) according to the single-layer balance (take $L = 1$ in (51); in particular $\alpha_1 \asymp \sqrt{h}$, clipped at α_0).*

Then:

(i) *Tangency-bad events can occur only in layer 1 (downstream crossings have a deterministic margin):*

$$\mathbb{P}(B_L(h, T; \alpha)) \leq \sum_{j=1}^{n_1} \mathbb{P}(B_{1,j}^{\text{mis}}(h, T)) + \frac{T}{2} \sum_{j=1}^{n_1} \rho_{\max,1,j}(T, \alpha_0) \alpha_1^2.$$

(ii) *For $\ell \geq 2$, the denominators $A_{\ell,j}^k$ are bounded below by α_ℓ^{MD} and the local deterministic Euler defect is $O(h)$ (rather than $O(h^{1/2})$), so downstream layers do not worsen the h -exponent in the STE recursion (41).*

(iii) *Consequently, for each fixed depth L , the good-set spike-time error exponent is the one from layer 1: if layer 1 has current noise, then $\Delta_L(T) = O(\sqrt{h \log(1/h)})$ up to multiplicative constants; if layer 1 is deterministic and mean-driven, then $\Delta_L(T) = O(h)$. The pruning bound for terminal-time observables inherits the same h -exponents, up to the mismatch probability from Lemma 3.16. Depth affects only multiplicative constants through weights and spike counts.*

Remark 3.32 (Relation to the fully mean-driven case). If *all* layers are deterministic and have a uniform transversality margin, then one can take all α_ℓ fixed and recover the deterministic (order-1) spike-time accuracy of forward Euler. In contrast, with Brownian current noise in a layer the crossing speed can be arbitrarily small with positive probability, so a.s. uniform transversality is generally unavailable; our α -splitting framework is designed for this stochastic setting.

We end the discussion of strong error for feedforward networks with the following remark:

Remark 3.33 (Spikes versus the classical 1/2 strong order). For smooth SDEs with Lipschitz coefficients, Euler–Maruyama has mean-square error $O(h)$ (RMS order 1/2) for the state at a fixed time. In the present hybrid setting, the subthreshold dynamics is still smooth and contributes the same $O(h)$ mean-square term, but the spike map depends on a *hitting time* and includes a *discontinuous reset*. Spike-time sensitivity introduces the random inverse factor $1/A$ with $A = I - I_{\text{th}}$ the crossing speed. The boundary-flux estimate implies that truncated inverse-speed moments diverge only logarithmically, so on the strong good set all squared error terms are of the form h times polynomials of $\log(1/h)$ (or iterated logs), i.e. “almost” the usual 1/2 strong behavior.

The remaining subtlety is the terminal-time mismatch layer: even when spike times are accurate, grid-based detection can change whether a spike is counted before or after the observation time T if an exact spike lies within $O(\sqrt{h \log(1/h)})$ of T . This produces an additional pruning term of size $\mathbb{P}(N^h(T) \neq N(T)) = O(\sqrt{h \log(1/h)})$ (Lemma 3.16), which can dominate for discontinuous terminal observables and yields the familiar $(h \log(1/h))^{1/4}$ RMS scaling.

4 Weak error: order 1 with explicit dependence on depth, time, and weights

Weak error cannot be controlled by pruning: missed/extra spikes must be handled directly. We therefore use a backward equation / semigroup argument with a probability-flow bound in a boundary strip.

4.1 State space, spike maps, and the exact Markov semigroup

Let $\mathcal{I} := \{(\ell, j) : 1 \leq \ell \leq L, 1 \leq j \leq n_\ell\}$ and $N := \sum_{\ell=1}^L n_\ell$. Write the network state as $x = (v, I) \in \mathbb{R}^{2N}$ with coordinates $(v_{\ell,j}, I_{\ell,j})_{(\ell,j) \in \mathcal{I}}$. Define the interior (subthreshold) domain

$$\mathsf{D} := \{x = (v, I) \in \mathbb{R}^{2N} : v_{\ell,j} < V_{\text{th}} \text{ for all } (\ell, j) \in \mathcal{I}\}.$$

For each neuron $p = (\ell, i) \in \mathcal{I}$ define the threshold surface

$$\Sigma_p := \{x \in \bar{\mathsf{D}} : v_{\ell,i} = V_{\text{th}}\}.$$

Spike map (reset + feedforward synaptic jump). When neuron $p = (\ell, i)$ spikes, it resets its own voltage and (if $\ell \leq L - 1$) produces an instantaneous current jump in layer $\ell + 1$. Define $\mathcal{R}_p : \bar{\mathsf{D}} \rightarrow \mathsf{D}$ by:

(i) $(\mathcal{R}_p x)_{v_{\ell,i}} := V_r,$

(ii) if $\ell \leq L - 1$, then for each $j \in \{1, \dots, n_{\ell+1}\},$

$$(\mathcal{R}_p x)_{I_{\ell+1,j}} := I_{\ell+1,j} + W_{ji}^{\ell, \ell+1},$$

(iii) all other coordinates are unchanged.

Exact process and semigroup. Let $X(t) = (V(t), I(t))$ be the exact network process: between spikes it solves (1)–(2), and when $X(t^-) \in \Sigma_p$ it jumps to $X(t^+) = \mathcal{R}_p(X(t^-))$. For bounded measurable $\Phi : \mathsf{D} \rightarrow \mathbb{R}$, define

$$(P_{s,t}\Phi)(x) := \mathbb{E}[\Phi(X(t)) \mid X(s) = x], \quad 0 \leq s \leq t.$$

4.2 EM one-step operator

Fix $h > 0$ and grid times $t_m := mh$. Given $x \in \mathsf{D}$ at time t_m , define the EM pre-update

$$v_{\ell,j}^{\text{pre}} = v_{\ell,j} + h \left(-\frac{1}{\tau_v} (v_{\ell,j} - V_r) + I_{\ell,j} \right), \quad I_{\ell,j}^{\text{pre}} = I_{\ell,j} - \frac{h}{\tau_c} (I_{\ell,j} - b_{\ell,j}(t_m)) + \frac{\sigma_{\ell,j}}{\tau_c} \Delta B_{\ell,j,m},$$

with independent $\Delta B_{\ell,j,m} \sim \mathcal{N}(0, h)$. Define the grid spike set

$$\mathcal{S}^{\text{grid}}(x) := \{p = (\ell, i) \in \mathcal{I} : v_{\ell,i}^{\text{pre}} \geq V_{\text{th}}\}.$$

Apply all spike maps at the grid endpoint:

$$x^{\text{post}} = \left(\prod_{p \in \mathcal{S}^{\text{grid}}(x)} \mathcal{R}_p \right) (v^{\text{pre}}, I^{\text{pre}}).$$

Define the EM one-step operator

$$(Q_h \Psi)(x) := \mathbb{E}[\Psi(x^{\text{post}})].$$

4.3 Backward value function and transmission at threshold

Fix $T = Mh$ and $\Phi \in C_b^4(\mathsf{D})$. Define

$$u(t, x) := (P_{t,T}\Phi)(x) = \mathbb{E}[\Phi(X(T)) \mid X(t) = x], \quad 0 \leq t \leq T.$$

On D , u solves the backward Kolmogorov equation $\partial_t u + \mathcal{L}_t u = 0$, $u(T, \cdot) = \Phi$, where the interior generator is

$$\mathcal{L}_t \varphi = \sum_{(\ell,j) \in \mathcal{I}} \left(-\frac{1}{\tau_v} (v_{\ell,j} - V_r) + I_{\ell,j} \right) \partial_{v_{\ell,j}} \varphi + \sum_{(\ell,j) \in \mathcal{I}} \left(-\frac{1}{\tau_c} (I_{\ell,j} - b_{\ell,j}(t)) \right) \partial_{I_{\ell,j}} \varphi + \sum_{(\ell,j) \in \mathcal{I}} \frac{\sigma_{\ell,j}^2}{2\tau_c^2} \partial_{I_{\ell,j} I_{\ell,j}} \varphi. \quad (53)$$

Transmission (gluing) at threshold for $t < T$. For $t < T$ and boundary states $x \in \Sigma_p$ reachable by upward crossing, the exact process jumps immediately $x \mapsto \mathcal{R}_p x$, hence

$$u(t, x) = u(t, \mathcal{R}_p x), \quad x \in \Sigma_p, \quad t < T. \quad (54)$$

4.4 Quantities controlling the weak constant

Layer rate bounds. Let $\Delta N_\ell(m)$ be the total number of exact spikes in layer ℓ during step m :

$$\Delta N_\ell(m) := \sum_{i=1}^{n_\ell} (N_{\ell,i}(t_{m+1}) - N_{\ell,i}(t_m)).$$

Assume there exist finite constants $R_\ell(T)$ such that for all m with $t_{m+1} \leq T$,

$$\mathbb{E}[\Delta N_\ell(m)] \leq R_\ell(T) h, \quad \ell = 1, \dots, L. \quad (55)$$

Weight norm for a single presynaptic spike. A spike of presynaptic neuron i in layer ℓ adds the i -th column of $W^{\ell, \ell+1}$ to the current vector of layer $\ell + 1$. Define the column-sum norm

$$\|W^{\ell, \ell+1}\|_1 := \max_{1 \leq i \leq n_\ell} \sum_{j=1}^{n_{\ell+1}} |W_{ji}^{\ell, \ell+1}|. \quad (56)$$

Boundary strip bound near threshold. For each neuron $p = (\ell, i)$ let $\varrho_p(v, t)$ be the marginal density of $v_p(t)$ (assume it exists). Assume (cf. Lemma 3.11 for a conservative explicit bound in a time-homogeneous OU surrogate setting).

$$\sup_{t \in [0, T]} \sup_{y \in [0, 1]} \varrho_p(V_{\text{th}} - y, t) \leq \rho_{\max, p}^V(T). \quad (57)$$

Crossing velocity moments. For each neuron p , define the upward velocity

$$a_p(x) := -\frac{1}{\tau_v} (v_p - V_r) + I_p, \quad a_p^+(x) := \max\{a_p(x), 0\}.$$

Assume

$$A_{2,p}(T) := \sup_{t \in [0, T]} \mathbb{E}[(a_p^+(X(t)))^2] < \infty. \quad (58)$$

Backward derivative bounds. Assume $u \in C^{1,4}([0, T] \times \mathbb{D})$ with bounded derivatives up to order 4. Define

$$M_v(T) := \sup_{t \in [0, T]} \max_{p \in \mathcal{I}} \|\partial_{v_p} u(t, \cdot)\|_\infty, \quad M_I(T) := \sup_{t \in [0, T]} \|\nabla_I u(t, \cdot)\|_\infty. \quad (59)$$

4.5 Two core lemmas: timing/decay vs. missed/extra spikes

Lemma 4.1 (Timing/decay defect due to off-grid synaptic jump times). *Fix a layer transition $\ell \rightarrow \ell + 1$ and a time step $[t_m, t_{m+1}]$. Condition on an exact spike of a presynaptic neuron in layer ℓ occurring at time $\tau \in (t_m, t_{m+1})$. At time t_{m+1} , shifting the synaptic jump time from τ to t_{m+1} changes the postsynaptic current vector in layer $\ell + 1$ (in l^1) by at most*

$$\frac{h}{\tau_c} \|W^{\ell, \ell+1}\|_1.$$

Consequently, for $f = u(t_{m+1}, \cdot)$, the one-step weak contribution from timing/decay across all spikes satisfies

$$\text{Timing/decay defect in step } m \leq \frac{h^2}{\tau_c} M_I(T) \sum_{\ell=1}^{L-1} R_\ell(T) \|W^{\ell, \ell+1}\|_1. \quad (60)$$

Proof. A jump applied at τ contributes at t_{m+1} with a factor $e^{-(t_{m+1}-\tau)/\tau_c}$. Shifting it to t_{m+1} changes the contribution by $|W|(1 - e^{-(t_{m+1}-\tau)/\tau_c}) \leq |W| h/\tau_c$. Summing over postsynaptic indices gives the l^1 bound $\frac{h}{\tau_c} \|W^{\ell, \ell+1}\|_1$ per presynaptic spike. Using $|f(x) - f(y)| \leq M_I(T) \|I_x - I_y\|_1$ and $\mathbb{E}[\Delta N_\ell(m)] \leq R_\ell(T)h$ yields (60). \square

Lemma 4.2 (Missed/extra spike-map decisions: boundary strip bound). *Fix a neuron $p \in \mathcal{I}$ and define, for $t < T$, the jump discrepancy function*

$$g_p(t, x) := u(t, \mathcal{R}_p x) - u(t, x).$$

Then $g_p(t, x) = 0$ for $x \in \Sigma_p$ (transmission (54)), and for interior states

$$|g_p(t, x)| \leq \|\partial_{v_p} u(t, \cdot)\|_\infty (V_{\text{th}} - v_p). \quad (61)$$

Define the spike-inducing strip

$$\mathcal{S}_{p,h}(t_m) := \left\{ x \in \mathbb{D} : 0 < V_{\text{th}} - v_p \leq h a_p^+(x) \right\}.$$

Then, for $t_{m+1} < T$,

$$\mathbb{E}[|g_p(t_{m+1}, X(t_m))| \mathbb{1}_{\{X(t_m) \in \mathcal{S}_{p,h}(t_m)\}}] \leq \frac{h^2}{2} M_v(T) \rho_{\max,p}^V(T) A_{2,p}(T). \quad (62)$$

Proof. Let $\pi_p x$ denote the boundary projection replacing v_p by V_{th} and leaving other coordinates unchanged. Because \mathcal{R}_p overwrites v_p , $\mathcal{R}_p x = \mathcal{R}_p(\pi_p x)$, and transmission gives $u(t, \pi_p x) = u(t, \mathcal{R}_p(\pi_p x)) = u(t, \mathcal{R}_p x)$ for $t < T$. Thus $g_p(t, x) = u(t, \pi_p x) - u(t, x)$ and (61) follows by the mean value theorem.

On $\mathcal{S}_{p,h}(t_m)$, let $y := V_{\text{th}} - v_p \in (0, h a_p^+(x)]$. Using (61) and the density bound (57),

$$\begin{aligned} \mathbb{E}[|g_p(t_{m+1}, X(t_m))| \mathbb{1}_{X(t_m) \in \mathcal{S}_{p,h}}] &\leq M_v(T) \mathbb{E}[(V_{\text{th}} - v_p) \mathbb{1}_{\{0 < V_{\text{th}} - v_p \leq h a_p^+\}}] \\ &\leq M_v(T) \rho_{\max,p}^V(T) \mathbb{E}\left[\int_0^{h a_p^+} y dy\right] = \frac{h^2}{2} M_v(T) \rho_{\max,p}^V(T) \mathbb{E}[(a_p^+)^2] \leq \frac{h^2}{2} M_v(T) \rho_{\max,p}^V(T) A_{2,p}(T). \end{aligned}$$

\square

4.6 One-step and global weak error bounds

Lemma 4.3 (One-step weak defect). *Let $t_{m+1} < T$ and set $f = u(t_{m+1}, \cdot)$. Assume the interior diffusion EM truncation yields the standard bound*

$$\sup_{x \in \mathbb{D}} \left| (Q_h^{\text{diff}} - P_{t_m, t_{m+1}}^{\text{diff}}) f(x) \right| \leq C_{\text{diff}}(T) h^2,$$

where Q_h^{diff} and P^{diff} denote one-step operators for the diffusion part without threshold/jumps. Then

$$\left| \mathbb{E}[u(t_{m+1}, X_{m+1}^h) - u(t_m, X_m^h)] \right| \leq h^2 \left(C_{\text{diff}}(T) + \frac{M_I(T)}{\tau_c} \sum_{\ell=1}^{L-1} R_\ell(T) \|W^{\ell, \ell+1}\|_1 + \frac{M_v(T)}{2} \sum_{p \in \mathcal{I}} \rho_{\max,p}^V(T) A_{2,p}(T) \right) \quad (63)$$

Proof. Decompose the one-step defect into: (i) interior diffusion truncation, (ii) synaptic timing/decay (Lemma 4.1), and (iii) missed/extra spike-map decisions (Lemma 4.2) summed over neurons p . \square

Theorem 4.4 (Global weak order 1 with explicit T - L scaling). *Let $T = Mh$ and $\Phi \in C_b^4(\mathbb{D})$. Assume Lemma 4.3 holds for steps $m = 0, \dots, M - 2$. Then*

$$\left| \mathbb{E}[\Phi(X(T))] - \mathbb{E}[\Phi(X^h(T))] \right| \leq Th C_{\text{weak}}(T, L, W) + C_{\text{term}}(T)h, \quad (64)$$

where

$$C_{\text{weak}}(T, L, W) := C_{\text{diff}}(T) + \frac{M_I(T)}{\tau_c} \sum_{\ell=1}^{L-1} R_\ell(T) \|W^{\ell, \ell+1}\|_1 + \frac{M_v(T)}{2} \sum_{p \in \mathcal{I}} \rho_{\max, p}^V(T) A_{2, p}(T), \quad (65)$$

and $C_{\text{term}}(T)$ controls the final step (where $u(T, \cdot) = \Phi$ and transmission need not hold). If Φ is spike-map compatible at T (i.e. $\Phi(x) = \Phi(\mathcal{R}_p x)$ for $x \in \Sigma_p$), then $C_{\text{term}}(T) = 0$.

Proof. Use the telescoping identity

$$\mathbb{E}[\Phi(X(T))] - \mathbb{E}[\Phi(X^h(T))] = \sum_{m=0}^{M-1} \mathbb{E}[u(t_{m+1}, X_{m+1}^h) - u(t_m, X_m^h)].$$

Apply Lemma 4.3 to $m = 0, \dots, M - 2$ to obtain $(M - 1)h^2 C_{\text{weak}}$ and bound the final step by $C_{\text{term}}(T)h$. \square

Remark 4.5 (Linear growth in L under uniform bounds). If $R_\ell(T) \leq R_{\max}(T)$, $\|W^{\ell, \ell+1}\|_1 \leq \mathcal{W}_1$, and $\rho_{\max, p}^V(T) A_{2, p}(T)$ is uniformly bounded and $N = \sum_\ell n_\ell \lesssim L$, then $C_{\text{weak}}(T, L, W)$ grows at most linearly in L . Thus the weak error scales like $O(Th)$ with linear-in- L constants under uniform controls.

5 Dynamical stability and Lyapunov exponents

This section studies *long-time* stability under *common-noise coupling* and clarifies how stability interacts with strong-error accumulation. We integrate (i) a deterministic integrate-and-fire (IF) warm-up (monotonicity/interlacing and finite-time spike-time sensitivity) and (ii) a general IF Lyapunov-exponent theorem based on saltation factors and stationary boundary flux, then specialize to the current-based LIF neuron and finally to feedforward networks.

5.1 Common-noise coupling and what “stability” means

Fix a single neuron or a feedforward network as in Section 2. Consider two copies $X(t)$ and $\tilde{X}(t)$ driven by the *same* Brownian motions $\{B_{\ell, j}\}$ and, in the network setting, by their own internally generated spike trains. We call this a *common-noise coupling*. Write $\delta v_{\ell, j}(t) = v_{\ell, j}(t) - \tilde{v}_{\ell, j}(t)$ and similarly for currents.

Because the reset map is discontinuous, L^∞ -type path metrics are misleading: even a small spike-time shift produces an $O(1)$ pointwise difference on a short *misalignment window* (see Lemma 3.19 and the discussion in Section 3.6). A more robust stability notion is based on (i) spike-time perturbations and/or (ii) time-integrated errors (e.g. L_t^1), which “pay” only the window length.

The natural infinitesimal stability quantity is the *top Lyapunov exponent* for perturbations in voltage along a typical trajectory, defined (when it exists) by

$$\lambda_v := \lim_{T \rightarrow \infty} \frac{1}{T} \log \frac{|\delta v(T^+)|}{|\delta v(0^+)|},$$

under common-noise coupling and an infinitesimal initial perturbation. The key fact is that, between spikes, voltage perturbations contract (for LIF) at rate e^{-t/τ_v} , while each spike produces

a multiplicative *saltation factor* due to the dependence of the spike time on the perturbation (cf. [4]).

To motivate (and to reuse later), we start with a deterministic 1D IF warm-up, which is also a useful pathwise template because in the common-noise setting one may condition on the input path.

5.2 Warm-up: deterministic 1D IF with common input

We summarize and integrate deterministic results (monotonicity/interlacing and finite-time spike-time sensitivity) in a form aligned with our notation.

5.2.1 Model and spike times

Let $x(t) \in [0, 1)$ solve the deterministic IF dynamics

$$\dot{x}(t) = f(x(t)) + I(t), \quad x(t) < 1, \quad (66)$$

with reset rule

$$x(t^-) = 1 \Rightarrow x(t^+) = 0. \quad (67)$$

Assume

$$f \in C^1([0, 1]), \quad f'(x) \leq 0 \text{ for all } x \in [0, 1], \quad (68)$$

and $I \in L^1_{\text{loc}}(\mathbb{R}_+)$ (measurable input). Given $x(0) = x_0 \in [0, 1)$, define spike times recursively:

$$s^1(x_0) := \inf\{t > 0 : x(t) = 1\}, \quad s^{k+1}(x_0) := \inf\{t > s^k(x_0) : x(t) = 1\},$$

with the convention $\inf \emptyset = \infty$. Let $N(T; x_0) := \sum_{k \geq 1} \mathbb{1}_{\{s^k(x_0) \leq T\}}$.

Remark 5.1 (Why L^∞ is not the right stability metric). Even with identical input $I(t)$, a small initial perturbation can produce an $O(1)$ *pointwise* difference because one trajectory spikes earlier and resets while the other has not yet spiked. However, this discrepancy persists only on an interval of length comparable to the spike-time shift. Thus time-integrated metrics (and spike-time metrics) capture the correct smallness. This is the same “misalignment window” mechanism used in the strong-error propagation analysis (Section 3.6).

5.2.2 Order preservation and contraction between spikes

Let $x(t; s, \xi)$ denote the (subthreshold) ODE solution of (66) on an interval where $x < 1$, starting at time s from $x(s) = \xi \in [0, 1)$. If $x_1(t) = x(t; s, \xi_1)$ and $x_2(t) = x(t; s, \xi_2)$ with $\xi_1 \geq \xi_2$, then by comparison (one-dimensional monotonicity),

$$x_1(t) \geq x_2(t) \quad \text{for all times before the first threshold hit of either solution.} \quad (69)$$

Moreover, letting $e(t) := x_1(t) - x_2(t) \geq 0$, we have $\dot{e}(t) = f(x_1(t)) - f(x_2(t))$ and $f' \leq 0$ implies $\dot{e}(t) \leq 0$, hence

$$0 \leq x_1(t) - x_2(t) \leq \xi_1 - \xi_2 \quad \text{for all times before the first threshold hit.} \quad (70)$$

5.2.3 Monotonicity and (mean-driven) Lipschitz bounds for spike times

Assumption 5.2 (Mean-driven transversality for deterministic input). There exists a constant $a_* > 0$ such that

$$f(1) + \operatorname{ess\,inf}_{t \geq 0} I(t) \geq a_* > 0. \quad (71)$$

Theorem 5.3 (Spike times vs. initial condition: monotonicity, right continuity, and Lipschitz bounds). *Assume (68). Then for each fixed $k \geq 1$, the map $x_0 \mapsto s^k(x_0)$ is nonincreasing and right-continuous on $[0, 1)$.*

If in addition Assumption 5.2 holds, then all spike times are finite ($s^k(x_0) < \infty$ for every k), and for any $\delta > 0$ with $x_0 + \delta < 1$,

$$|s^k(x_0 + \delta) - s^k(x_0)| \leq \frac{1}{a_*} S_*^{k-1} |\delta|, \quad S_* := \frac{f(0) + \operatorname{ess\,inf}_{t \geq 0} I(t)}{f(1) + \operatorname{ess\,inf}_{t \geq 0} I(t)} \geq 1. \quad (72)$$

Proof. Step 1: monotonicity. Fix $\delta > 0$ with $x_0 + \delta < 1$, and let $x^\delta(t)$ denote the solution from $x_0 + \delta$, $x(t)$ the solution from x_0 , under the same input $I(t)$. By (69), $x^\delta(t) \geq x(t)$ until one hits threshold, so $s^1(x_0 + \delta) \leq s^1(x_0)$. Restarting at reset and iterating yields $s^k(x_0 + \delta) \leq s^k(x_0)$ for all k .

Step 2: right continuity. Monotonicity of $s^k(\cdot)$ implies existence of one-sided limits; right continuity follows from standard monotone-function properties together with the fact that threshold is hit from below and solutions depend continuously on initial data for ODEs between events.

Step 3: Lipschitz under mean-driven transversality. Under (71), for any subthreshold state $x(t) \in [0, 1]$ we have $\dot{x}(t) = f(x(t)) + I(t) \geq f(1) + \operatorname{ess\,inf} I \geq a_*$. Hence the first spike time satisfies the crude bound

$$|s^1(x_0 + \delta) - s^1(x_0)| \leq \frac{|\delta|}{a_*}.$$

To propagate to later spikes we use the *saltation factor* for 1D IF. At a spike time $s = s^k(x_0)$, a perturbation in initial condition produces a spike-time shift Δs that is proportional to the pre-spike perturbation divided by the threshold velocity $f(1) + I(s)$. Immediately after reset, the state is 0, but the post-reset state at a common clock time differs because one trajectory has advanced for an extra Δs under velocity $f(0) + I(s)$. Thus the magnitude of the post-spike perturbation is multiplied by

$$S(I(s)) := \frac{f(0) + I(s)}{f(1) + I(s)}.$$

Since $f' \leq 0$, $f(0) \geq f(1)$ and $S(\cdot) \geq 1$. Under (71) and $I(s) \geq \operatorname{ess\,inf} I$, we have $S(I(s)) \leq S_*$ with S_* defined in (72). Iterating over $k - 1$ spikes gives the stated Lipschitz bound. \square

Remark 5.4 (Geometric sensitivity vs. Lyapunov growth). The factor S_*^{k-1} in (72) is the finite-time counterpart of a Lyapunov exponent: roughly, if the spike count up to time T satisfies $N(T) \approx rT$, then $S_*^{N(T)} \approx e^{r(\log S_*)T}$. The next subsection makes this precise in a stationary stochastic setting.

5.2.4 Interlacing and spike-count mismatch is at most one

A crucial structural consequence of (69)–(70) is that two solutions driven by the *same* input cannot drift arbitrarily far apart in spike count.

Lemma 5.5 (Interlacing of spike times). *Assume (68). Consider two solutions x_A, x_B of (66)–(67) with the same input $I(t)$ and initial data $x_A(0) \geq x_B(0)$. Then their spike times interlace:*

$$s_A^1 \leq s_B^1 \leq s_A^2 \leq s_B^2 \leq \dots,$$

with the understanding that if one side has fewer than k spikes then the corresponding time is ∞ . In particular, for every $T \geq 0$,

$$|N_A(T) - N_B(T)| \leq 1. \quad (73)$$

Proof. We sketch the standard induction argument. Since $x_A(0) \geq x_B(0)$, order preservation implies the first threshold hit of x_A occurs no later than that of x_B , hence $s_A^1 \leq s_B^1$. At time s_A^1 , x_A resets to 0, while $x_B(s_A^1) \in [0, 1)$, so now $x_B(s_A^1) \geq x_A(s_A^1) = 0$. Applying order preservation from s_A^1 onward yields $s_B^1 \leq s_A^2$, and repeating gives the interlacing chain. The spike-count bound (73) is immediate from interlacing. \square

Remark 5.6 (What interlacing does *not* prevent). Interlacing controls spike *count* mismatch, but it does not guarantee that a trajectory that missed a spike will eventually “catch up” in a way that makes trajectories close pointwise. For example, if after one trajectory spikes the input becomes subthreshold, the lagging trajectory may never spike (a permanent loss, producing $O(1)$ separation). This phenomenon is relevant when interpreting pruning-type strong bounds: in some regimes a missed spike truly can be irrecoverable.

5.2.5 Spike-count bounds from input integrals

The deterministic notes also provide useful spike-count bounds, which become rate bounds once inputs are bounded.

Proposition 5.7 (Spike-count upper bound). *Assume (68) and $I \in L^1([0, T])$. Then any solution satisfies*

$$N(T; x_0) \leq x_0 + \int_0^T (I(s) + f(0))_+ ds. \quad (74)$$

In particular, if $I(s) \leq I_{\max}$ a.e. on $[0, T]$, then

$$N(T; x_0) \leq (I_{\max} + f(0))_+ T + x_0. \quad (75)$$

Proof. Between spikes, $x(t)$ increases at speed $\dot{x} = I(t) + f(x(t)) \leq I(t) + f(0)$ since f is nonincreasing. Each spike requires an increment of 1 in x . Summing increments over interspike intervals yields the integral bound (74). \square

Remark 5.8 (Relevance for our network constants). Bounds like (75) provide explicit deterministic rate controls under bounded inputs. In our strong/weak network bounds, such rate controls enter via spike-load parameters and stepwise rate bounds.

5.3 A general 1D IF Lyapunov exponent theorem

We now state a general Lyapunov-exponent theorem for one-dimensional IF models with an *autonomous* (stationary ergodic) input process. The theorem isolates (i) continuous-time contraction/expansion between spikes and (ii) discrete spike-induced expansion via a saltation factor. It subsumes the LIF formula used later.

5.3.1 Stochastic IF with autonomous input

Let $(\Omega, \mathcal{F}, \mathbb{P})$ carry a stationary ergodic process $I(t)$ with càdlàg paths. Consider the IF dynamics

$$\dot{x}(t) = f(x(t)) + I(t), \quad x(t) < 1, \quad x(t^-) = 1 \Rightarrow x(t^+) = 0, \quad (76)$$

with $f \in C^1([0, 1])$. Assume spikes are *transversal* almost surely: whenever $x(t^-) = 1$ at a spike time $t = s^k$,

$$f(1) + I(s^{k-}) > 0. \quad (77)$$

Let $\{s^k\}_{k \geq 1}$ be the spike times and $N(t) = \sum_k \mathbb{1}_{\{s^k \leq t\}}$. Define the *saltation factor* (ratio of post-/pre-spike infinitesimal perturbations)

$$S(I) := \frac{f(0) + I}{f(1) + I}, \quad \text{defined for } f(1) + I > 0. \quad (78)$$

This is the 1D specialization of the saltation matrix for event-driven/hybrid flows; for spiking neurons it appears explicitly in [4].

5.3.2 Invariant measure and boundary flux

Assume that the joint process $(x(t), I(t))$ on $\{x < 1\}$ with reinjection at $x = 0$ is positive recurrent and admits a stationary ergodic distribution π_∞ on $\mathbb{D} := [0, 1) \times \mathbb{R}$. Assume moreover that the stationary law admits a density $\rho_\infty(x, I)$ that is bounded in a neighborhood of $(1, I)$ for I near the tangency set $\{f(1) + I = 0\}$. In the Markov case (e.g. I an OU diffusion), the corresponding stationary Fokker–Planck equation implies a stationary *outflow boundary flux* through $x = 1$ given by

$$J_\infty(I) = (f(1) + I) \rho_\infty(1, I) \mathbb{1}_{\{f(1)+I>0\}}. \quad (79)$$

More generally (beyond Markov), J_∞ can be understood as the stationary *Palm* measure of I at spike times; for our purposes the Markov/flux setting is sufficient.

Theorem 5.9 (General 1D IF Lyapunov exponent via stationary bulk measure and boundary flux). *Assume:*

- (i) $f \in C^1([0, 1])$ and spikes are transversal a.s. in the sense of (77);
- (ii) $(x(t), I(t))$ is stationary ergodic with invariant density $\rho_\infty(x, I)$ on $[0, 1) \times \mathbb{R}$;
- (iii) the stationary boundary flux measure exists and is given by (79);
- (iv) (integrability) $\rho_\infty(1, I)$ is locally bounded near the tangency set $f(1) + I = 0$.

Then the top Lyapunov exponent for infinitesimal perturbations in the x -direction under common-input coupling equals

$$\lambda_x = \int_{[0,1) \times \mathbb{R}} f'(x) \rho_\infty(x, I) dx dI + \int_{\mathbb{R}} J_\infty(I) \log S(I) dI, \quad S(I) = \frac{f(0) + I}{f(1) + I}. \quad (80)$$

Moreover, the boundary integral is finite despite the logarithmic singularity at $f(1) + I \downarrow 0$.

Proof. Step 1: multiplicative decomposition of the tangent dynamics. Consider the derivative $D(t) := \partial_{x_0} x(t)$ along a fixed input path. Between spikes, D solves $\dot{D}(t) = f'(x(t))D(t)$, hence $D(t) = \exp(\int_{s^k}^t f'(x(u)) du) D(s^{k+})$ on each interspike interval. At a spike time $s = s^k$, the perturbation affects the spike time itself; the standard saltation calculation (or [4]) yields

$$D(s^+) = S(I(s^-)) D(s^-), \quad S(I) = \frac{f(0) + I}{f(1) + I}.$$

Combining yields, for any $T > 0$,

$$\log |D(T^+)| = \log |D(0^+)| + \int_0^T f'(x(t)) dt + \sum_{k: s^k \leq T} \log S(I(s^{k-})). \quad (81)$$

Step 2: ergodic limits. Divide (81) by T and let $T \rightarrow \infty$. Stationary ergodicity gives

$$\frac{1}{T} \int_0^T f'(x(t)) dt \rightarrow \int f'(x) \rho_\infty(x, I) dx dI \quad \text{a.s.}$$

For the spike sum, define the random measure $\mu_T(dI) := \frac{1}{T} \sum_{k: s^k \leq T} \delta_{I(s^{k-})}(dI)$. Under stationarity/ergodicity, μ_T converges (in the Cesàro/Palm sense) to the stationary spike flux measure $J_\infty(I) dI$ characterized by (79), i.e.

$$\frac{1}{T} \sum_{k: s^k \leq T} \varphi(I(s^{k-})) \rightarrow \int \varphi(I) J_\infty(I) dI \quad \text{for bounded continuous } \varphi.$$

Applying this with $\varphi = \log S$ (justified by the integrability step below) yields the second term in (80), and the initial factor $\log |D(0^+)|/T \rightarrow 0$.

Step 3: finiteness of the logarithmic singularity. Let $a := f(1) + I$ and consider the near-tangency regime $a \downarrow 0^+$. Then $\log S(I) = \log \frac{f(0)+I}{f(1)+I} = \log \frac{f(0)-f(1)+a}{a} \sim \log \frac{1}{a}$, while the flux density has a factor a : $J_\infty(I) = (f(1) + I)\rho_\infty(1, I)\mathbb{1}_{\{a>0\}} = a\rho_\infty(1, f(1) + a)$. If $\rho_\infty(1, \cdot)$ is locally bounded, then near $a = 0$ the integrand behaves like $a \log(1/a)$, which is integrable: $\int_0^\alpha a \log(1/a) da < \infty$. Thus the boundary integral in (80) is finite. \square

Remark 5.10 (A useful crude upper bound). Using $\log(1+x) \leq x$ one gets

$$0 \leq (f(1) + I) \log S(I) = (f(1) + I) \log\left(1 + \frac{f(0) - f(1)}{f(1) + I}\right) \leq f(0) - f(1).$$

Hence

$$\int J_\infty(I) \log S(I) dI \leq (f(0) - f(1)) \int_{\{f(1)+I>0\}} \rho_\infty(1, I) dI,$$

showing finiteness under minimal boundary-density integrability assumptions.

5.4 Single current-based LIF neuron: explicit λ and bounds

We specialize Theorem 5.9 to the current-based LIF neuron used throughout this paper. Recall the single-neuron dynamics (1)–(2) with reset (3). For the *voltage* equation, conditional on the current path $I(t)$ the voltage is a 1D IF equation with drift $f(v) = -(v - V_r)/\tau_v$ and input $I(t)$. Thus $f'(v) = -1/\tau_v$ and

$$f(V_r) = 0, \quad f(V_{th}) = -\frac{V_{th} - V_r}{\tau_v} = -I_{th}, \quad I_{th} := \frac{V_{th} - V_r}{\tau_v}.$$

The corresponding saltation factor at a spike with pre-spike current $I(s^-)$ is

$$S(I) = \frac{f(V_r) + I}{f(V_{th}) + I} = \frac{I}{I - I_{th}}, \quad I > I_{th}, \quad (82)$$

in agreement with [4].

Assume the stationary subthreshold density $\rho_\infty(v, I)$ exists on $\{v < V_{th}\}$ and is bounded near (V_{th}, I_{th}) . Then the stationary boundary flux is

$$J_\infty(I) = (I - I_{th})\rho_\infty(V_{th}, I)\mathbb{1}_{\{I>I_{th}\}}.$$

Theorem 5.11 (Single-neuron LIF Lyapunov exponent (voltage direction)). *Under stationarity/ergodicity and boundedness of $\rho_\infty(V_{th}, I)$ near $I = I_{th}$, the voltage Lyapunov exponent under common-noise coupling equals*

$$\lambda_v = -\frac{1}{\tau_v} + \int_{I>I_{th}} (I - I_{th}) \rho_\infty(V_{th}, I) \log\left(\frac{I}{I - I_{th}}\right) dI = -\frac{1}{\tau_v} + \int_{\mathbb{R}} J_\infty(I) \log S(I) dI, \quad (83)$$

and the integral is finite despite the logarithmic singularity of $\log \frac{I}{I - I_{th}}$ at $I \downarrow I_{th}$.

Proof. Apply Theorem 5.9 with $f'(v) = -1/\tau_v$ and $S(I)$ given by (82). Integrability follows as in Theorem 5.9 because the flux density has the factor $(I - I_{th})$ and $\rho_\infty(V_{th}, I)$ is locally bounded near $I = I_{th}$. \square

Remark 5.12 (Upper bounds in terms of boundary density). Using $\log(1+x) \leq x$ with $x = I_{th}/(I - I_{th})$,

$$0 \leq (I - I_{th}) \log\left(\frac{I}{I - I_{th}}\right) = (I - I_{th}) \log\left(1 + \frac{I_{th}}{I - I_{th}}\right) \leq I_{th}.$$

Thus

$$\lambda_v \leq -\frac{1}{\tau_v} + I_{\text{th}} \int_{I > I_{\text{th}}} \rho_\infty(V_{\text{th}}, I) dI. \quad (84)$$

A sharper bound splits $I \in (I_{\text{th}}, I_{\text{th}} + \alpha)$ and $I \geq I_{\text{th}} + \alpha$: on $(I_{\text{th}}, I_{\text{th}} + \alpha)$ use $\rho_\infty(V_{\text{th}}, I) \leq \rho_{\text{max}}$ (Section 3.3) to get an explicit $O(\alpha^2 \log(1/\alpha))$ contribution; on $[I_{\text{th}} + \alpha, \infty)$ the logarithm is uniformly bounded.

Remark 5.13 (Connection to finite-time spike-time sensitivity (warm-up theorem)). Assumption 5.2 corresponds for LIF (in normalized voltage coordinates) to a uniform transversality margin $I(t) - I_{\text{th}} \geq \alpha > 0$. Then Theorem 5.3 yields geometric spike-time sensitivity with factor $S_* = \frac{I_{\text{th}} + \alpha}{\alpha}$, matching the saltation factor bound in (82).

5.5 Feedforward networks: upstream exponents force downstream divergence

We now incorporate the crucial feedforward point: *even if a downstream neuron is contractive for a frozen presynaptic spike train, a positive upstream Lyapunov exponent produces exponentially diverging spike times, which generate exponentially diverging synaptic currents downstream.*

5.5.1 A forcing estimate: spike-time divergence \Rightarrow current divergence

Consider one presynaptic neuron (layer 1) and one postsynaptic neuron (layer 2) coupled by a weight w with exponential synapse kernel $K(t; s) = e^{-(t-s)/\tau_c} \mathbb{1}_{\{t \geq s\}}$. Let $\{s_1^k\}$ and $\{\tilde{s}_1^k\}$ be the spike times of the two copies of neuron 1 (with matched indices), and define $\varepsilon_1^k := \tilde{s}_1^k - s_1^k$.

Lemma 5.14 (Upstream spike-time divergence forces downstream current divergence). *Assume spike indices of neuron 1 remain matched up to time T . Let I_2^{ff} and \tilde{I}_2^{ff} be the feedforward parts of the postsynaptic currents driven by N_1 and \tilde{N}_1 . Then*

$$\int_0^T |I_2^{\text{ff}}(t) - \tilde{I}_2^{\text{ff}}(t)| dt \leq 2|w| \sum_{k: s_1^k \leq T} |\varepsilon_1^k|. \quad (85)$$

Consequently, by Lemma 3.21, the induced voltage difference satisfies

$$\sup_{t \leq T} |v_2(t) - \tilde{v}_2(t)| \leq \int_0^T |I_2(t) - \tilde{I}_2(t)| dt \lesssim 2|w| \sum_{k: s_1^k \leq T} |\varepsilon_1^k| + (\text{local terms}). \quad (86)$$

Proof. This is the single-synapse specialization of the misalignment-window estimate: apply Lemma 3.19 to each shifted presynaptic spike and sum. Then use Lemma 3.21 to convert an L_t^1 current difference to a voltage sup-norm bound. \square

Remark 5.15 (Exponential upstream STE implies exponential downstream forcing). If $|\varepsilon_1^k|$ grows like $e^{\lambda_1 t}$ along spike index k (e.g. $\max_{s_1^k \leq T} |\varepsilon_1^k| \asymp e^{\lambda_1 T}$) and the spike count grows at most linearly $N_1(T) \lesssim T$, then the RHS of (85) is $\lesssim T e^{\lambda_1 T}$. Thus downstream differences cannot decay faster than the upstream exponent, up to polynomial factors.

5.5.2 A max-rule for layerwise Lyapunov exponents

We now formulate a clean propagation statement in the feedforward setting. For each layer ℓ , define the *diagonal* (frozen-input) exponent $\lambda_\ell^{\text{diag}}$: this is the top Lyapunov exponent of layer ℓ under common-noise coupling when the presynaptic spike trains from layers $< \ell$ are treated as *fixed external inputs shared by both copies*. In particular, for a single neuron in layer ℓ with frozen input, $\lambda_\ell^{\text{diag}}$ is given by the single-neuron flux/saltation formula (Theorem 5.11), with the stationary boundary density induced by that frozen input.

Let λ_ℓ be the actual layer- ℓ exponent within the full coupled feedforward network (so presynaptic spikes may differ).

Theorem 5.16 (Feedforward max-type propagation of Lyapunov exponents). *Assume a stationary regime in which:*

- (i) all layerwise diagonal exponents $\lambda_\ell^{\text{diag}}$ are well defined,
- (ii) spike times remain transversal and spike indices can be matched between the two coupled copies,
- (iii) each layer $\ell \geq 2$ receives at least one nonzero synaptic weight from layer $\ell - 1$.

Then for $\ell = 2, \dots, L$,

$$\lambda_\ell \geq \max\{\lambda_\ell^{\text{diag}}, \lambda_{\ell-1}\}. \quad (87)$$

Moreover, under a Lipschitz forcing structure of the synaptic input map (as quantified by Lemma 5.14 and its multi-neuron extension), one also has the upper bound

$$\lambda_\ell \leq \max\{\lambda_\ell^{\text{diag}}, \lambda_{\ell-1}\}, \quad (88)$$

and hence the exact max rule

$$\lambda_\ell = \max\{\lambda_\ell^{\text{diag}}, \lambda_{\ell-1}\}. \quad (89)$$

In particular, if $\lambda_1 > 0$ then $\lambda_\ell \geq \lambda_1$ for all ℓ .

Proof. We sketch the argument. Lower bounds: $\lambda_\ell \geq \lambda_\ell^{\text{diag}}$ by choosing initial perturbations supported in layer ℓ only. Also Lemma 5.14 shows that perturbations in layer $\ell - 1$ force layer ℓ at the same exponential rate (up to subexponential factors), hence $\lambda_\ell \geq \lambda_{\ell-1}$. Upper bound: a variation-of-constants estimate for the forced variational system yields $\|\delta X_\ell(t)\| \lesssim e^{\lambda_\ell^{\text{diag}} t} \|\delta X_\ell(0)\| + \int_0^t e^{\lambda_\ell^{\text{diag}}(t-s)} \|\delta X_{\ell-1}(s)\| ds$, implying $\lambda_\ell \leq \max\{\lambda_\ell^{\text{diag}}, \lambda_{\ell-1}\}$. \square

Remark 5.17 (Where the warm-up interlacing can help). For 1D IF driven by a *common* input and with $f' \leq 0$, Lemma 5.5 implies that spike-count mismatch is uniformly bounded by 1. This supports the matched-indices assumption above for single neurons and in regimes where effective order-preservation holds.

5.6 Implications for strong error accumulation in time

On the good event $G_L(h, T; \alpha)$ in the strong analysis (Section 3), spike indices are matched and crossings are transversal, so error propagation is governed by the local sensitivity of spike times and state variables. In this regime, the hybrid/common-noise Lyapunov exponent λ_ℓ derived above is the natural stability diagnostic: if $\lambda_\ell < 0$, small perturbations contract on average and the good-set strong error does not exhibit secular exponential growth.

The pruning decomposition used in Section 3, however, treats the bad set as *absorbing*: once a tangency or mismatch event occurs, we bound the error by a worst-case constant and do not attempt to re-couple. This design choice makes the bounds explicit, but it disconnects λ_ℓ from the *probability mass* of bad trajectories.

When $\lambda_\ell < 0$, many trajectories that temporarily enter a mismatch configuration are expected to *recover*. Intuitively, contraction reduces the probability that a one-step mismatch triggers a long cascade of subsequent mismatches: after a transient discrepancy, the common-noise flow pulls the two trajectories back together, making them “good again”. In 1D integrate-and-fire with a common input and $f' \leq 0$, interlacing (Lemma 5.5) already implies that spike-count mismatch is at most one; in such order-preserving settings, recovery after a transient mismatch is plausible unless the dynamics enters a subthreshold trapping regime (Remark 5.6). For networks, the same idea suggests that negative Lyapunov behavior should reduce the expected *time spent* in mismatch episodes, and hence reduce the contribution of bad trajectories in long-time strong error.

A sharper long-time theory would therefore replace the absorbing bad event by an entry/exit bookkeeping: one would track the stopping times at which the coupled trajectories leave G_L and (possibly) re-enter it, and bound the expected total time spent outside G_L . In such a framework, $\lambda_\ell < 0$ can enter explicitly through bounds on the tail of the recovery time. We do not pursue this non-pruning coupling here; accordingly, our pruning bounds should be read as conservative. They correctly identify the mechanisms that can destroy strong accuracy (near-tangential crossings and synchronous bursts) but do not exploit possible recovery in contractive regimes.

6 Recurrent networks: intuition and strong error bounds

6.1 Intuition: recurrence creates an effective depth through feedback loops

A recurrent spiking network can be unfolded in time. For a finite horizon, it behaves as a feedforward system until the influence of a spike traverses a directed synaptic loop and returns to a neuron already affected by that spike. If the shortest feedback loop has synaptic length L^* (number of synapses on the loop), then a single spike-time perturbation can be amplified over an *effective depth* comparable to L^* before closing the loop. In regimes with spike cascades (a nontrivial fraction of neurons fire within a short time window), the effective depth over $[0, T]$ can be much larger than the anatomical loop length, because many events occur in causal chains. This is precisely the mechanism by which pruning-based strong-error bounds can deteriorate rapidly in recurrent networks.

6.2 Model: recurrent current-based LIF network

We consider N_r neurons indexed by $i \in \{1, \dots, N_r\}$ with recurrent weight matrix $W \in \mathbb{R}^{N_r \times N_r}$. The continuous-time dynamics is

$$dv_i(t) = \left(-\frac{1}{\tau_v} (v_i(t) - V_r) + I_i(t) \right) dt, \quad v_i(t) < V_{\text{th}}, \quad (90)$$

$$dI_i(t) = -\frac{1}{\tau_c} (I_i(t) - b_i(t)) dt + \frac{\sigma_i}{\tau_c} dB_i(t) + \sum_{j=1}^{N_r} W_{ij} dN_j(t), \quad (91)$$

with instantaneous reset $v_i((s_i^k)^+) = V_r$ at each spike time s_i^k defined by upward threshold crossing. The threshold current is $I_{\text{th}} = (V_{\text{th}} - V_r)/\tau_v$ and the crossing speed is $A_i^k = I_i((s_i^k)^-) - I_{\text{th}}$.

The numerical method is Euler–Maruyama for I and forward Euler for v , with grid-based spike detection and reset (as in Section 2).

6.3 Scenario 1: deterministic mean-driven recurrent hybrid system ($\sigma \equiv 0$)

In this subsection we assume $\sigma_i \equiv 0$ for all i , so the network is a deterministic hybrid system.

6.3.1 Continuous variational flow

Let $x = (v, I) \in \mathbb{R}^{2N_r}$, where $v, I \in \mathbb{R}^{N_r}$. Between spikes, the Jacobian of the ODE is the constant block matrix

$$A = \begin{pmatrix} -\tau_v^{-1} I_{N_r} & I_{N_r} \\ 0 & -\tau_c^{-1} I_{N_r} \end{pmatrix}, \quad F(\Delta) := e^{A\Delta} = \begin{pmatrix} e^{-\Delta/\tau_v} I_{N_r} & B(\Delta) I_{N_r} \\ 0 & e^{-\Delta/\tau_c} I_{N_r} \end{pmatrix},$$

where

$$B(\Delta) = \int_0^\Delta e^{-(\Delta-s)/\tau_v} e^{-s/\tau_c} ds = \begin{cases} \frac{\tau_v \tau_c}{\tau_c - \tau_v} (e^{-\Delta/\tau_c} - e^{-\Delta/\tau_v}), & \tau_v \neq \tau_c, \\ \Delta e^{-\Delta/\tau_v}, & \tau_v = \tau_c. \end{cases}$$

6.3.2 Saltation matrix at a spike event

Let neuron p spike at time s . The event surface is $g_p(x) = v_p - V_{\text{th}} = 0$ with normal $n_p = e_{v_p}$. Denote the pre-spike speed $A_p = I_p(s^-) - I_{\text{th}}$. The reset map sets $v_p \mapsto V_r$ and adds the synaptic column jump $I \mapsto I + W_{:p}$. The saltation matrix S_p mapping δx^- to δx^+ at fixed global time is

$$S_p = \left(I_{2N_r} - e_{v_p} e_{v_p}^\top \right) + \frac{1}{A_p} u_p e_{v_p}^\top, \quad u_p = \begin{pmatrix} W_{:p} + I_p^- e_p \\ -\tau_c^{-1} W_{:p} \end{pmatrix}, \quad (92)$$

where $I_p^- = I_p(s^-)$ and e_p is the unit vector in the v -block at index p . Equivalently, acting on perturbations $(\delta v^-, \delta I^-)$,

$$\delta v^+ = \delta v^- - e_p \delta v_p^- + \frac{\delta v_p^-}{A_p} \left(W_{:p} + I_p^- e_p \right), \quad \delta I^+ = \delta I^- - \frac{\delta v_p^-}{\tau_c A_p} W_{:p}. \quad (93)$$

6.3.3 Hybrid fundamental matrix and a Lyapunov upper bound

Let $0 < s_1 < \dots < s_M \leq T$ be the spike-event times (across all neurons) and let p_m be the neuron spiking at s_m . The hybrid fundamental matrix is

$$\Phi_{\text{hyb}}(T, 0) = F(T - s_M) S_{p_M} F(s_M - s_{M-1}) \cdots S_{p_1} F(s_1). \quad (94)$$

Assumption 6.1 (Deterministic transversality). There exists $\alpha_* > 0$ such that at every spike event, $A_p \geq \alpha_*$.

Theorem 6.2 (Explicit hybrid fundamental matrix and an upper bound on λ_{hyb}). *Assume Assumption 6.1. Let $N_{\text{tot}}(T) = M$ be the total number of spike events in $[0, T]$ and $r_{\text{tot}}(T) = N_{\text{tot}}(T)/T$. Let $I_{\text{max}}(T) = \max_i \sup_{t \leq T} |I_i(t)|$ and $\|W\|_{\text{max}} = \max_{i,j} |W_{ij}|$. Then the saltation matrices satisfy the uniform bound (in the induced $\|\cdot\|_\infty$ matrix norm)*

$$\|S_p\|_\infty \leq \kappa_S(T), \quad \kappa_S(T) := \max \left\{ \frac{I_{\text{max}}(T) + \|W\|_{\text{max}}}{\alpha_*}, 1 + \frac{\|W\|_{\text{max}}}{\alpha_*}, 1 + \frac{\|W\|_{\text{max}}}{\tau_c \alpha_*} \right\}.$$

Moreover, since the continuous variational flow is exponentially stable, there exists a Lyapunov norm $\|\cdot\|_*$ such that $\|F(\Delta)\|_* \leq e^{-\Delta/\tau_{\text{max}}}$ with $\tau_{\text{max}} = \max\{\tau_v, \tau_c\}$. In that norm,

$$\|\Phi_{\text{hyb}}(T, 0)\|_* \leq e^{-T/\tau_{\text{max}}} \kappa_S(T)^{N_{\text{tot}}(T)}.$$

Consequently the top hybrid Lyapunov exponent satisfies

$$\lambda_{\text{hyb}} := \limsup_{T \rightarrow \infty} \frac{1}{T} \log \|\Phi_{\text{hyb}}(T, 0)\|_* \leq -\frac{1}{\tau_{\text{max}}} + \bar{r}_{\text{tot}} \log \kappa_S,$$

where $\bar{r}_{\text{tot}} = \limsup_{T \rightarrow \infty} r_{\text{tot}}(T)$ and $\kappa_S = \limsup_{T \rightarrow \infty} \kappa_S(T)$.

Remark 6.3 (Connection to cycle-gain amplification). The saltation structure (93) shows that each spike of neuron p injects its voltage perturbation δv_p^- into downstream currents and voltages through the synaptic column $W_{:p}$ with amplification proportional to $1/A_p$. This is the mechanism underlying the cycle-gain criterion: if a directed cycle C is repeatedly realized by the dynamics and the product of per-edge gains exceeds 1, then the spike-time Lyapunov exponent is forced positive.

6.3.4 Mean-driven deterministic numerics: error growth controlled by λ_{hyb}

We now make explicit how the deterministic dynamical stability rate (hybrid Lyapunov exponent) controls deterministic discretization error accumulation in a mean-driven regime.

Assumption 6.4 (No multiple spikes per neuron per time step). There exists $h_0 > 0$ such that for all $h \in (0, h_0)$ and for all neurons i , the exact trajectory has at most one spike in any interval $(t_m, t_{m+1}]$ of length h up to time T .

Theorem 6.5 (Deterministic mean-driven recurrent network: numerical error grows at rate λ_{hyb}). Assume $\sigma \equiv 0$, Assumption 6.1, and Assumption 6.4. Let $x(t) = (v(t), I(t))$ be the exact hybrid trajectory and let $x^h(t)$ be the time-driven Euler trajectory with grid-based reset, driven by the same initial data $x^h(0) = x(0)$. Assume the exact trajectory remains in a bounded set on $[0, T]$ (so all coefficients and event gains are uniformly bounded).

Then there exists $h_1 \in (0, h_0]$ such that for all $h \in (0, h_1)$:

(i) the exact and numerical spike sequences have the same event ordering (no missed/extra spikes);

(ii) for any $\varepsilon > 0$ there exists a constant $C_\varepsilon(T)$ such that the global state error satisfies

$$\sup_{t_m \leq T} \|x^h(t_m) - x(t_m)\|_* \leq C_\varepsilon(T) e^{(\lambda_{\text{hyb}} + \varepsilon)T} h; \quad (95)$$

(iii) in particular, the spike-time errors satisfy

$$\max_i \max_{k: s_i^k \leq T} \left| \hat{s}_i^k - s_i^k \right| \leq \frac{1}{\alpha_*} C_\varepsilon(T) e^{(\lambda_{\text{hyb}} + \varepsilon)T} h. \quad (96)$$

Consequently, if $\lambda_{\text{hyb}} < 0$ then the deterministic scheme is uniformly accurate in time ($O(h)$ as $T \rightarrow \infty$), whereas if $\lambda_{\text{hyb}} > 0$ deterministic errors can grow at most exponentially at rate λ_{hyb} .

Proof. Step 1: event matching for small h . Under Assumption 6.1 and Assumption 6.4, for h small the grid monitoring cannot miss a transversal spike: over each step the exact voltage crosses threshold with strictly positive speed bounded below by α_* , and the numerical voltage differs from the exact voltage by $O(h)$ over a step because the subthreshold dynamics is smooth. Thus for sufficiently small h the spike indicator on each step agrees, and since at most one spike per neuron can occur per step, event ordering is preserved.

Step 2: a hybrid variation-of-constants representation. Let $0 < s_1 < \dots < s_M \leq T$ be the exact spike-event times across all neurons and let p_m be the event neuron at s_m . Write $x_m^+ := x(s_m^+)$ and similarly $(x_m^h)^+$ for the numerical post-event state at the corresponding numerical event time (which is within $O(h)$ of s_m). On each inter-event interval, the exact flow is given by the linear map $F(\cdot)$ and the numerical flow differs by a local truncation of order $O(h)$ over the interval (Euler local defect integrated over time plus the $O(h)$ event time snapping). At each event, the exact and numerical resets differ by a linear saltation factor S_{p_m} plus an additional $O(h)$ defect due to snapping the spike time within the step.

Collecting these standard hybrid perturbation terms yields an error recursion of the form

$$e_m^+ = S_{p_m} F(s_m - s_{m-1}) e_{m-1}^+ + \eta_m, \quad \|\eta_m\|_* \leq C_{\text{loc}}(T) h,$$

with $e_m^+ = (x_m^h)^+ - x_m^+$ and $s_0 := 0$. Unrolling the recursion yields

$$e_M^+ = \Phi_{\text{hyb}}(T, 0) e_0^+ + \sum_{m=1}^M \Phi_{\text{hyb}}(T, s_m) \eta_m,$$

where $\Phi_{\text{hyb}}(T, s_m)$ is the hybrid fundamental matrix from s_m to T . Since $e_0^+ = 0$, we obtain

$$\|e_M^+\|_* \leq \sum_{m=1}^M \|\Phi_{\text{hyb}}(T, s_m)\|_* \|\eta_m\|_* \leq C_{\text{loc}}(T) h \sum_{m=1}^M \|\Phi_{\text{hyb}}(T, s_m)\|_*.$$

Step 3: growth control by λ_{hyb} . By the definition of λ_{hyb} as a top Lyapunov exponent, for any $\varepsilon > 0$ there exists $C_\varepsilon(T)$ such that $\|\Phi_{\text{hyb}}(t, s)\|_* \leq C_\varepsilon(T) e^{(\lambda_{\text{hyb}} + \varepsilon)(t-s)}$ for all $0 \leq s \leq t \leq T$. Thus

$$\|e_M^+\|_* \leq C_{\text{loc}}(T) h C_\varepsilon(T) \sum_{m=1}^M e^{(\lambda_{\text{hyb}} + \varepsilon)(T-s_m)} \leq C_\varepsilon(T) e^{(\lambda_{\text{hyb}} + \varepsilon)T} h,$$

after absorbing the finite sum into the constant (recall $M < \infty$ on $[0, T]$). This yields (95) at event times and hence at grid times.

Step 4: spike-time error. Under transversality $A_p \geq \alpha_*$, the spike-time sensitivity bound (Lemma 3.4) gives $|\hat{s} - s| \leq \alpha_*^{-1} \sup |v^h - v|$, and $\sup |v^h - v|$ is controlled by $\|x^h - x\|_*$, yielding (96). \square

Remark 6.6 (Interpretation). Theorem 6.5 is the deterministic analog of the “stability vs. long-time error” discussion in Section 5.6: in deterministic mean-driven recurrence, the hybrid Lyapunov exponent directly controls numerical error accumulation. This mechanism is fundamentally different from pruning-based bounds, where bad-event probability terms cannot be canceled by contraction on good paths.

6.4 Scenario 2: noisy recurrent networks under rate and density bounds

We now return to $\sigma_i > 0$ and treat recurrent networks by the same spike-time / pruning framework as in the feedforward case, but with loop amplification encoded via rate and graph bounds.

6.4.1 Rate bounds and synchrony control

Let $\Delta N_{\text{tot}}(m) = \sum_{j=1}^{N_r} (N_j(t_{m+1}) - N_j(t_m))$ be the total number of exact spikes in step m . We assume the existence of finite constants $R_{\text{net}}(T)$ and $R_{\text{net},2}(T)$ such that

$$\mathbb{E}[\Delta N_{\text{tot}}(m)] \leq R_{\text{net}}(T) h, \quad \mathbb{E}[\Delta N_{\text{tot}}(m)(\Delta N_{\text{tot}}(m) - 1)] \leq R_{\text{net},2}(T) h^2, \quad (97)$$

Remark 6.7 (On $R_{\text{net}}(T)$ versus $R_{\text{net},2}(T)$). The two bounds in (97) encode different information and are not redundant. The first-moment bound $R_{\text{net}}(T)$ is implied, for instance, by deterministic firing-rate envelopes $r_j(t) \leq r_j^{\text{max}}(T)$ via $R_{\text{net}}(T) = \sum_j r_j^{\text{max}}(T)$. The second factorial-moment bound $R_{\text{net},2}(T)$ controls within-step *synchrony/burstiness*: by Markov’s inequality, $\mathbb{P}(\Delta N_{\text{tot}}(m) \geq 2) \leq \frac{1}{2} \mathbb{E}[\Delta N_{\text{tot}}(m)(\Delta N_{\text{tot}}(m) - 1)]$, so $R_{\text{net},2}(T)$ is exactly what limits the probability of multiple spikes in one step. Such control cannot be inferred from $R_{\text{net}}(T)$ alone, and it is precisely where synchronized regimes deteriorate time-driven error constants.

for all steps with $t_{m+1} \leq T$. Scenario R2 corresponds to moderate $R_{\text{net}}, R_{\text{net},2}$ (asynchronous, weak synchrony), while Scenario R4 has the same form but much larger constants (burstier synchrony).

6.4.2 Boundary density constants and their estimates

For each neuron i , define the boundary density constant (near tangency)

$$\rho_{\text{max},i}(T, \alpha_0) := \sup_{t \in [0, T]} \sup_{a \in [0, \alpha_0]} \rho_i(V_{\text{th}}, I_{\text{th}} + a, t),$$

and the voltage marginal bound near threshold

$$\rho_{\max,i}^V(T) := \sup_{t \in [0,T]} \sup_{y \in [0,1]} \varrho_i(V_{\text{th}} - y, t),$$

where ρ_i is the (v_i, I_i) subthreshold density and ϱ_i is the voltage marginal.

As in the feedforward analysis, $\rho_{\max,i}(T, \alpha_0)$ controls both the tangency mass and the log-truncated inverse moment of A_i^{-1} , while $\rho_{\max,i}^V(T)$ enters conservative strip-based density bounds (used later for weak error estimates). Our sharp spike-count mismatch bound is instead formulated in terms of rate and burst constants; see Lemma 3.16. In regimes with sufficiently strong independent Brownian noise in each current, hypoellipticity suggests these constants are finite; however they can become large (and can blow up in the small-noise limit) in bursty synchronized regimes.

A baseline explicit proxy and its limitation in recurrent networks. A convenient explicit proxy is obtained by *freezing* the recurrent input into an exogenous drift μ_i and approximating the current by a linear OU process (diffusion only in I_i):

$$dI_i = -\frac{1}{\tau_c}(I_i - \mu_i) dt + \frac{\sigma_i}{\tau_c} dB_i, \quad dv_i = \left(-\frac{1}{\tau_v}(v_i - V_r) + I_i\right) dt.$$

Its stationary density yields the baseline proxy estimates

$$\rho_{\max,i}(T, \alpha_0) \lesssim \frac{\sqrt{\tau_c}(\tau_c + \tau_v)}{\pi \sigma_i^2 \tau_v^{3/2}}, \quad \rho_{\max,i}^V(T) \lesssim \frac{\sqrt{\tau_c + \tau_v}}{\sqrt{\pi} \sigma_i \tau_v}. \quad (98)$$

A sharper (rate- and weight-dependent) proxy replaces σ_i by an effective diffusion $\sigma_{\text{eff},i}$,

$$\sigma_{\text{eff},i}^2(t) \approx \sigma_i^2 + \kappa \tau_c^2 \sum_{j=1}^{N_r} W_{ij}^2 r_j(t),$$

which is the standard diffusion approximation of synaptic shot noise in asynchronous regimes.

Remark 6.8 (Important caveat: recurrent vs. feedforward.). The OU surrogate treats the input $\mu_i(t)$ (and the rate field $r_j(t)$ used in $\sigma_{\text{eff},i}$) as *given* and, crucially, *independent* of the intrinsic Brownian motion B_i . This independence is natural in feedforward networks and can be a good approximation for large recurrent networks in weakly correlated (asynchronous / mean-field) regimes, where the contribution of a single neuron's noise to its own net input is negligible. In genuinely recurrent, strongly correlated regimes, however, $\mu_i(t)$ depends on the network spike trains and therefore inherits correlations with B_i . In particular, in tight E–I balance or near-synchronous cascade regimes, recurrent input can partially cancel intrinsic noise and produce an *effective* variance $\sigma_{\text{eff},i}^2(t)$ that is small, leading to very slow threshold crossings and potentially near-singular voltage marginals near V_{th} . For this reason, in the recurrent sections we treat $\rho_{\max,i}(T, \alpha_0)$ and $\rho_{\max,i}^V(T)$ primarily as assumptions (or as empirically estimated constants), and we use (98) only as a baseline proxy when such decoupling is justified.

6.4.3 Tangency probability and spike-count mismatch probability

For tangency, the boundary flux argument yields (as in Section 3.3):

$$\mathbb{P}(B_i^{\text{tan}}(\alpha, T)) \leq \frac{T}{2} \rho_{\max,i}(T, \alpha_0) \alpha^2, \quad (99)$$

where $B_i^{\text{tan}}(\alpha, T)$ is the event that neuron i has a spike with speed $A_i < \alpha$.

For mismatch, we use the *horizon-based* spike-count mismatch event

$$B_i^{\text{mis}}(h, T) := \{N_i^h(T) \neq N_i(T)\},$$

which treats false positives and false negatives symmetrically and ignores transient stepwise discrepancies that catch up before the observation time. Assume the local rate and burst controls (27)–(28) and the sub-Gaussian spike-time tail (29) hold for neuron i . Then Lemma 3.16 yields, for any $\delta \in (0, 1]$,

$$\mathbb{P}(B_i^{\text{mis}}(h, T)) \leq 2r_i^{\text{max}}(T)\delta + 4R_i^{(2)}(T)\delta^2 + C_i^{\text{err}}(T)\exp\left(-c_{\text{sg}}\frac{\delta^2}{h}\right), \quad (100)$$

and, with the canonical choice $\delta = \delta_h := \kappa\sqrt{h\log(1/h)}$,

$$\mathbb{P}(B_i^{\text{mis}}(h, T)) \lesssim r_i^{\text{max}}(T)\sqrt{h\log(1/h)} + R_i^{(2)}(T)h\log(1/h) + C_i^{\text{err}}(T)h^{c_0}, \quad c_0 := c_{\text{sg}}\kappa^2. \quad (101)$$

Importantly, this mismatch bound is independent of the tangency cutoff α .

6.4.4 Good-set STE inequality and explicit loop-length truncation

Fix truncation thresholds $\alpha_i \in (0, \alpha_0]$. Let $G(h, T; \alpha)$ be the event that all spikes up to T satisfy $A_i^k \geq \alpha_i$ and that spike counts match at the observation time (no horizon mismatch), i.e. $N_i^h(T) = N_i(T)$ for every neuron i .

For each neuron j , define the (good-set) spike-load bound

$$\Lambda_j^{\text{rec}}(T) := \sup_{\omega \in G(h, T; \alpha)} \#\{k : s_j^k(\omega) \leq T\}, \quad \Lambda_{\text{tot}}^{\text{rec}}(T) := \sum_{j=1}^{N_r} \Lambda_j^{\text{rec}}(T).$$

(For example, $\Lambda_j^{\text{rec}}(T) \leq r_j^{\text{max}}T$ on G if one has deterministic rate bounds.)

Define the good-set RMS STE vector $\Delta(T) \in \mathbb{R}^{N_r}$ by

$$\Delta_i(T) := \max_{k: s_i^k \leq T} \mathbb{E}[|\varepsilon_i^k|^2 \mathbf{1}_G]^{1/2}.$$

As in the feedforward analysis, one obtains a linear propagation inequality with a local term plus a synaptic misalignment term. Using Lemma 3.8 to control inverse crossing speeds, define the layerwise inverse-moment factors

$$\mathbf{m}_i(T; \alpha_i) := \left(\frac{1}{\alpha_0^2} + T \rho_{\text{max}, i}(T, \alpha_0) \log \frac{\alpha_0}{\alpha_i} \right)^{1/2},$$

and the local coefficients

$$a_i(T) := C_i^{\text{loc}}(T) h^{1/2} \mathbf{m}_i(T; \alpha_i).$$

Define the nonnegative gain matrix $G(T) \in \mathbb{R}^{N_r \times N_r}$ with entries

$$G_{ij}(T) := 2 \mathbf{m}_i(T; \alpha_i) |W_{ij}| \Lambda_j^{\text{rec}}(T). \quad (102)$$

Lemma 6.9 (Recurrent good-set STE inequality). *On $G(h, T; \alpha)$, the STE vector satisfies*

$$\Delta(T) \leq a(T) + G(T) \Delta(T) \quad \text{componentwise.} \quad (103)$$

Proof. This is the recurrent analogue of Theorem 3.24, with the uniform $1/\alpha_i$ bound replaced by the log-truncated inverse moment. For each neuron i and each of its spikes, Lemma 3.4

gives $|\varepsilon_i^k| \leq (A_i^k)^{-1} \sup_{t \in [s_i^k - h, s_i^k + h]} |v_i(t) - v_i^h(t)|$. Squaring, multiplying by $\mathbf{1}_G$, and applying Cauchy–Schwarz yields

$$\mathbb{E}[|\varepsilon_i^k|^2 \mathbf{1}_G]^{1/2} \leq \left(\mathbb{E}[(A_i^k)^{-2} \mathbf{1}_{\{A_i^k \geq \alpha_i\}} \mathbf{1}_G] \right)^{1/2} \mathbb{E} \left[\sup_{t \in [s_i^k - h, s_i^k + h]} |v_i(t) - v_i^h(t)|^2 \mathbf{1}_G \right]^{1/2}.$$

Lemma 3.8 (with $\rho_{\max, i}$) bounds the first factor by $\mathfrak{m}_i(T; \alpha_i)$. For the second factor, the subthreshold strong error on $[0, T]$ yields the local contribution $C_i^{\text{loc}}(T)h^{1/2}$. Each presynaptic neuron j contributes via synaptic jump misalignment: the total L_t^1 jump discrepancy up to time T is bounded by $2|W_{ij}| \sum_{k: s_j^k \leq T} |\varepsilon_j^k|$ and hence by $2|W_{ij}| \Lambda_j^{\text{rec}}(T) \Delta_j(T)$ on G . Collecting terms and taking the maximum over k yields (103). \square

The inequality (103) is algebraic. To obtain a finite-horizon bound without imposing a contraction condition on $G(T)$, we exploit that causality in time bounds the maximum number of synaptic “hops” through which a single local defect can propagate by time T . This yields an explicit loop-length truncation.

Definition 6.10 (Shortest directed cycle length). Let $\mathcal{G} = (\{1, \dots, N_r\}, E)$ be the directed synaptic graph where $(j \rightarrow i) \in E$ iff $W_{ij} \neq 0$. Define $L^* \in \{2, 3, \dots\} \cup \{\infty\}$ as the length of the shortest directed cycle in \mathcal{G} (take $L^* = \infty$ if \mathcal{G} is acyclic).

Assumption 6.11 (Effective causal depth on the good set). Fix $\omega \in G(h, T; \alpha)$ and consider a *time-ordered influence chain* of spikes

$$(j_0, k_0) \rightarrow (j_1, k_1) \rightarrow \dots \rightarrow (j_m, k_m),$$

meaning: (i) for each $r = 1, \dots, m$ there is a directed synaptic edge $j_{r-1} \rightarrow j_r$ (so $W_{j_r j_{r-1}} \neq 0$), and (ii) the spike times are strictly increasing and lie within the horizon, $s_{j_{r-1}}^{k_{r-1}}(\omega) < s_{j_r}^{k_r}(\omega) \leq T$. Assume there exists an integer $K_{\text{eff}}(T) \leq \Lambda_{\text{tot}}^{\text{rec}}(T)$ such that no such chain on $G(h, T; \alpha)$ has length $m > K_{\text{eff}}(T)$.

Remark 6.12 (Interpreting $K_{\text{eff}}(T)$). $K_{\text{eff}}(T)$ is an *effective depth in time*: it bounds how many successive synaptic transmissions a local defect can traverse by time T . A crude deterministic bound is $K_{\text{eff}}(T) = \Lambda_{\text{tot}}^{\text{rec}}(T)$ (each transmission requires a spike). In asynchronous regimes with moderate within-step rates and weak synchrony, one expects $K_{\text{eff}}(T) = O(T)$; a simple proxy is $K_{\text{eff}}(T) \approx R_{\text{net}}(T)T$. In bursty synchronized regimes $K_{\text{eff}}(T)$ can be much larger, reflecting deep event cascades.

Theorem 6.13 (Explicit loop-truncated good-set STE bound). *Assume Assumption 6.11. Then on the good set,*

$$\Delta(T) \leq \left(\sum_{k=0}^{K_{\text{eff}}(T)} G(T)^k \right) a(T), \quad \text{componentwise.} \quad (104)$$

Consequently, in the induced $\|\cdot\|_\infty$ norm,

$$\|\Delta(T)\|_\infty \leq \left\| \sum_{k=0}^{K_{\text{eff}}(T)} G(T)^k \right\|_\infty \|a(T)\|_\infty. \quad (105)$$

Moreover, let L^* be the shortest directed cycle length from Definition 6.10. If $L^* = \infty$ (acyclic synaptic graph), then the truncated Neumann series can be bounded directly by

$$\left\| \sum_{k=0}^{K_{\text{eff}}(T)} G(T)^k \right\|_\infty \leq \sum_{k=0}^{K_{\text{eff}}(T)} \|G(T)\|_\infty^k. \quad (106)$$

If $L^* < \infty$, write $K_{\text{eff}}(T) = M(T)L^* + R(T)$ with $R(T) \in \{0, \dots, L^* - 1\}$. Then we have the loop-block estimate

$$\left\| \sum_{k=0}^{K_{\text{eff}}(T)} G(T)^k \right\|_{\infty} \leq \left(\sum_{r=0}^{L^*-1} \|G(T)\|_{\infty}^r \right) \sum_{m=0}^{M(T)} \|G(T)^{L^*}\|_{\infty}^m, \quad (107)$$

and, in particular, if $\|G(T)^{L^*}\|_{\infty} < 1$, then

$$\left\| \sum_{k=0}^{K_{\text{eff}}(T)} G(T)^k \right\|_{\infty} \leq \left(\sum_{r=0}^{L^*-1} \|G(T)\|_{\infty}^r \right) \frac{1}{1 - \|G(T)^{L^*}\|_{\infty}}, \quad (108)$$

uniformly in $K_{\text{eff}}(T)$.

Proof. Step 1: truncation by causal depth. Iterate the inequality (103) by substitution:

$$\Delta \leq a + G\Delta \leq a + G(a + G\Delta) = a + Ga + G^2\Delta \leq \dots \leq \sum_{k=0}^K G^k a + G^{K+1}\Delta.$$

Under Assumption 6.11, the remainder term $G^{K+1}\Delta$ is absent on the good set once $K \geq K_{\text{eff}}(T)$: each multiplication by G corresponds to taking one synaptic predecessor, so $(G^{K+1}\Delta)_i$ expands into contributions along directed, time-ordered influence chains of length $K+1$ ending at neuron i . By definition of $K_{\text{eff}}(T)$, such chains do not exist on $G(h, T; \alpha)$ for $K = K_{\text{eff}}(T)$. Therefore, on G the Neumann series truncates and (104) holds. Taking $\|\cdot\|_{\infty}$ gives (105).

Step 2: series bounds (acyclic vs. cyclic). If $L^* = \infty$ (acyclic synaptic graph), then submultiplicativity gives

$$\left\| \sum_{k=0}^{K_{\text{eff}}} G^k \right\|_{\infty} \leq \sum_{k=0}^{K_{\text{eff}}} \|G\|_{\infty}^k,$$

which is (106) (with $G = G(T)$ and $K_{\text{eff}} = K_{\text{eff}}(T)$).

If $L^* < \infty$, write $K_{\text{eff}} = ML^* + R$ with $R \in \{0, \dots, L^* - 1\}$ and decompose the series into blocks:

$$\sum_{k=0}^{K_{\text{eff}}} G^k = \sum_{m=0}^{M-1} \sum_{r=0}^{L^*-1} G^{mL^*+r} + \sum_{r=0}^R G^{ML^*+r} = \sum_{m=0}^M G^{mL^*} \left(\sum_{r=0}^{L^*-1} G^r \right),$$

where the last identity uses a conservative completion of the final block. Taking $\|\cdot\|_{\infty}$ and using submultiplicativity yields (107). If $\|G^{L^*}\|_{\infty} < 1$, the geometric series gives (108). \square

6.4.5 Pruning strong bound for noisy recurrent networks

Let $X(T)$ be any bounded network output functional such that on G the strong error is Lipschitz in the spike-time metric: $\|X^h(T) - X(T)\| \leq L_X \|\Delta(T)\|_{\infty}$. Then the pruning decomposition yields

$$\mathbb{E} \|X^h(T) - X(T)\|^2 \leq L_X^2 \|\Delta(T)\|_{\infty}^2 + C_{\max}^2 \mathbb{P}(G(h, T; \alpha)^c), \quad (109)$$

where

$$\mathbb{P}(G(h, T; \alpha)^c) \leq \sum_{i=1}^{N_r} \mathbb{P}(B_i^{\text{tan}}(\alpha_i, T)) + \sum_{i=1}^{N_r} \mathbb{P}(B_i^{\text{mis}}(h, T)).$$

The tangency terms are controlled by (99), while the spike-count mismatch terms are controlled by (101) (equivalently, Lemma 3.16). Combining with Theorem 6.13 yields a fully explicit strong bound in terms of $(\alpha, W, \Lambda^{\text{rec}}, L^*, K_{\text{eff}}, \rho_{\max}, r^{\max}, R^{(2)})$. Importantly, the mismatch contribution is independent of the tangency cutoff α and therefore does not enter the α -balancing.

How L^* , $K_{\text{eff}}(T)$, and synaptic weights enter the good-set term. To make the dependence transparent, consider a uniform choice $\alpha_i \equiv \alpha$ and crude uniform bounds $\|W\|_\infty \leq \mathcal{W}$, $\Lambda_j^{\text{rec}}(T) \leq \Lambda^{\text{rec}}(T)$, and $C_i^{\text{loc}}(T) \leq C_{\text{loc}}(T)$. Let $\rho_{\text{max}}(T, \alpha_0) := \max_i \rho_{\text{max},i}(T, \alpha_0)$ and define $\mathbf{m}(T; \alpha)$ as in (48) with this recurrent ρ_{max} . Then $\|a(T)\|_\infty \lesssim C_{\text{loc}}(T) h^{1/2} \mathbf{m}(T; \alpha)$ and

$$\|G(T)\|_\infty \lesssim 2\mathcal{W} \Lambda^{\text{rec}}(T) \mathbf{m}(T; \alpha).$$

The good-set term in (109) is therefore controlled by

$$\|\Delta(T)\|_\infty \lesssim C_{\text{loc}}(T) h^{1/2} \mathbf{m}(T; \alpha) \left\| \sum_{k=0}^{K_{\text{eff}}(T)} G(T)^k \right\|_\infty.$$

If $\|G(T)\|_\infty < 1$ (a loop-stable regime), the Neumann series is uniformly bounded and the good-set RMS scales like \sqrt{h} up to the mild (logarithmic) α -dependence contained in $\mathbf{m}(T; \alpha)$. In contrast, if $\|G(T)\|_\infty \gtrsim 1$, a crude bound gives $\left\| \sum_{k=0}^{K_{\text{eff}}(T)} G^k \right\|_\infty \lesssim \|G\|_\infty^{K_{\text{eff}}(T)}$ and hence

$$\|\Delta(T)\|_\infty \lesssim C_{\text{loc}}(T) h^{1/2} \mathbf{m}(T; \alpha) (2\mathcal{W} \Lambda^{\text{rec}}(T) \mathbf{m}(T; \alpha))^{K_{\text{eff}}(T)}.$$

This highlights the roles of (i) the effective event depth $K_{\text{eff}}(T)$ (how many synaptic transmissions can occur along a causal influence chain), (ii) the loop length L^* via the block bound (107) (how often the shortest feedback cycle can be traversed), and (iii) the synaptic weight scale \mathcal{W} and the spike-load $\Lambda^{\text{rec}}(T)$. In typical asynchronous regimes one expects $\Lambda^{\text{rec}}(T) = O(T)$, while $\mathbf{m}(T; \alpha)$ grows at least like $(T \rho_{\text{max}} \log(\alpha_0/\alpha))^{1/2}$ in fluctuation-driven settings; consequently the constants can grow rapidly in T unless additional loop-stability or mixing control is available.

Remark 6.14 (Interpreting L^* through weak dependence and density control). When the current of every neuron is driven by IID white noise, even with the log-truncated inverse moment, $\mathbf{m}(T; \alpha)$ typically increases as $\alpha \downarrow 0$, so one should not assume a loop-contraction condition such as $\|G(T)^{L^*}\|_\infty < 1$ holds uniformly as $h \rightarrow 0$. This could only happen when all the neurons on the loop (except for the first one) are mean-driven. Hence, a more robust interpretation of L^* is probabilistic: the recurrent network can be viewed as feedforward along a time-ordered synaptic influence chain until the chain closes, i.e. until $j_m = j_0$. When L^* is large, self-feedback requires many hops and the resulting synaptic input $\mu_j(t)$ is often approximately exogenous to neuron j (in asynchronous/mixing regimes), so the boundary-density constants ρ_{max} and ρ_{max}^V are better controlled and the proxy bound (98) is more plausible. When L^* is small, however, this decoupling is not guaranteed and (98) may fail in strongly correlated or synchronized regimes.

Remark 6.15 (A crude α -balancing rule under deep cascades). In the crude regime $\left\| \sum_{k=0}^{K_{\text{eff}}(T)} G^k \right\|_\infty \lesssim \|G\|_\infty^{K_{\text{eff}}(T)}$, the good-set MSE inherits the factor $\|G(T)\|_\infty^{2K_{\text{eff}}(T)}$. Since $\|G(T)\|_\infty$ contains $\mathbf{m}(T; \alpha)$, the cutoff α enters only through the logarithmic dependence in $\mathbf{m}(T; \alpha)$ (contrast with the algebraic $1/\alpha$ worst-case amplification). Balancing the good-set term against the tangency mass $\sum_i \mathbb{P}(B_i^{\text{tan}}) \lesssim T \rho_{\text{max}}(T, \alpha_0) \alpha^2$ therefore leads to an *implicit* log-balance, analogous to (51) but with the power of $\mathbf{m}(T; \alpha)$ amplified by $K_{\text{eff}}(T)$ through the gain series. In particular, for fixed T this balancing does not typically change the leading \sqrt{h} scaling of the good-set term (only polylogarithmic factors), but it can produce extremely large constants when $K_{\text{eff}}(T)$ is large.

Remark 6.16 (Why bursty synchrony is disastrous for pruning bounds). In bursty regimes, the causal depth $K_{\text{eff}}(T)$ can be large (deep cascades), and loop-block growth (107) can produce large amplification even on the good set. Moreover, density bounds $\rho_{\text{max},i}$ and $\rho_{\text{max},i}^V$ can become extremely large in small-noise synchronized regimes (and may approach singularities as noise $\downarrow 0$), so that both the tangency mass and the mismatch constants (r^{max} and $R^{(2)}$) can deteriorate. Both effects worsen the strong bound and can force the pruning estimate to become vacuous in strongly synchronized regimes.

Remark 6.17 (Spikes and strong order in recurrent networks). The recurrent strong bounds have the same structural origin as in the feedforward case (Remark 3.33): subthreshold Euler error is $O(h)$ in mean square, while the spike map contributes inverse crossing speeds and a pruning probability term. Ignoring the terminal-time mismatch layer, the squared strong error is again h times polylogarithmic factors in h , so the effective strong order remains close to the classical Euler–Maruyama $1/2$ rate.

What changes in recurrence is not the local h -scaling but the *amplification mechanism*: feedback loops can recycle spike-time perturbations, and the good-set recursion is controlled by the shortest directed cycle length and by weight/rate constants (Theorem 6.13). As in the feedforward setting, discontinuous terminal observables also inherit the mismatch term $\mathbb{P}(N^h(T) \neq N(T)) = O(\sqrt{h \log(1/h)})$, which can dominate the pruning bound when spikes occur near the observation time.

7 Recurrent networks: weak error under rate and density bounds

Weak error concerns expectations and therefore cannot be handled by pruning. We adapt the backward-Kolmogorov / Markov-operator argument from Section 4 and make the dependence on the recurrent rate bounds R_{net} and $R_{\text{net},2}$ explicit.

7.1 Spike maps and a weight norm for recurrent jumps

When neuron p spikes, it resets v_p and adds the synaptic column $W_{\cdot,p}$ to the current vector. The recurrent spike map \mathcal{R}_p therefore shifts the *entire* current vector. The relevant weight norm for the one-step timing/decay defect is the column-sum norm

$$\|W\|_1 := \max_{1 \leq p \leq N_r} \sum_{i=1}^{N_r} |W_{ip}|.$$

A single spike of neuron p changes the current vector in l^1 by at most $\|W\|_1$.

7.2 Rate bounds and second factorial moment

Let $\Delta N_{\text{tot}}(m) = \sum_{j=1}^{N_r} (N_j(t_{m+1}) - N_j(t_m))$. Assume there exist finite constants $R_{\text{net}}(T)$ and $R_{\text{net},2}(T)$ such that

$$\mathbb{E}[\Delta N_{\text{tot}}(m)] \leq R_{\text{net}}(T) h, \quad \mathbb{E}[\Delta N_{\text{tot}}(m)(\Delta N_{\text{tot}}(m) - 1)] \leq R_{\text{net},2}(T) h^2,$$

for all m with $t_{m+1} \leq T$. The first bound controls the expected number of spikes per step, while the second controls the probability of multiple spikes within a step (burst/synchrony).

7.3 One-step weak defect: explicit dependence on R_{net} and $R_{\text{net},2}$

Let $\Phi \in C_b^4(\mathbb{D})$ and let $u(t, x) = \mathbb{E}[\Phi(X(T)) \mid X(t) = x]$ be the backward value function, as in Section 4. Let

$$M_v(T) := \sup_{t \in [0, T]} \max_p \|\partial_{v_p} u(t, \cdot)\|_\infty, \quad M_I(T) := \sup_{t \in [0, T]} \|\nabla_I u(t, \cdot)\|_\infty.$$

Assume the voltage strip density constants $\rho_{\max, i}^V(T)$ exist, and define the velocity moments

$$A_{2,i}(T) := \sup_{t \in [0, T]} \mathbb{E}[(a_i^+(X(t)))^2], \quad a_i(x) = -\frac{1}{\tau_v}(v_i - V_r) + I_i, \quad a_i^+ = \max\{a_i, 0\}.$$

Lemma 7.1 (Recurrent one-step weak defect). *Fix a step m with $t_{m+1} < T$ and set $f = u(t_{m+1}, \cdot)$. Assume the interior diffusion EM truncation yields the standard bound $\sup_{x \in \mathbb{D}} |(Q_h^{\text{diff}} - P_{t_m, t_{m+1}}^{\text{diff}})f(x)| \leq C_{\text{diff}}(T)h^2$. Then the full one-step defect satisfies*

$$\begin{aligned} & |\mathbb{E}[u(t_{m+1}, X_{m+1}^h) - u(t_m, X_m^h)]| \leq \\ & h^2 \left(C_{\text{diff}}(T) + \frac{M_I(T)}{\tau_c} R_{\text{net}}(T) \|W\|_1 + \frac{M_v(T)}{2} \sum_{i=1}^{N_r} \rho_{\text{max},i}^V(T) A_{2,i}(T) + \|u\|_\infty R_{\text{net},2}(T) \right). \end{aligned} \quad (110)$$

Proof. Decompose the one-step defect into four contributions.

(i) *Interior diffusion truncation.* This is bounded by $C_{\text{diff}}(T)h^2$ by assumption.

(ii) *Synaptic timing/decay.* A single spike at time $\tau \in (t_m, t_{m+1})$ produces an exponential synaptic factor at t_{m+1} . Shifting the jump time to t_{m+1} changes each postsynaptic current by at most $|W_{ip}|(1 - e^{-(t_{m+1}-\tau)/\tau_c}) \leq |W_{ip}|h/\tau_c$. Summing over postsynaptic i yields an l^1 change $\leq (h/\tau_c)\|W\|_1$ per spike. By the Lipschitz bound in currents, $|f(x) - f(y)| \leq M_I(T)\|I_x - I_y\|_{l^1}$, and taking expectation over the number of spikes in the step gives the term $\frac{M_I(T)}{\tau_c} R_{\text{net}}(T)\|W\|_1 h^2$.

(iii) *Missed/extra spike-map decisions.* This is controlled exactly as in Lemma 4.2 by the boundary strip estimate, yielding $\frac{h^2}{2} M_v(T) \sum_i \rho_{\text{max},i}^V(T) A_{2,i}(T)$.

(iv) *Multiple spikes within one step.* On the event $\{\Delta N_{\text{tot}}(m) \geq 2\}$ we use the trivial bound $|u(t_{m+1}, \cdot)| \leq \|u\|_\infty$. By Markov's inequality and the second factorial moment bound,

$$\mathbb{P}(\Delta N_{\text{tot}}(m) \geq 2) \leq \frac{1}{2} \mathbb{E}[\Delta N_{\text{tot}}(m)(\Delta N_{\text{tot}}(m) - 1)] \leq \frac{1}{2} R_{\text{net},2}(T)h^2.$$

Absorbing constants yields the term $\|u\|_\infty R_{\text{net},2}(T)h^2$. Summing (i)–(iv) gives (110). \square

7.4 Global weak order 1 with explicit rate dependence

Theorem 7.2 (Recurrent global weak order 1 with explicit $R_{\text{net}}, R_{\text{net},2}$ scaling). *Let $T = Mh$ and $\Phi \in C_b^4(\mathbb{D})$. Assume Lemma 7.1 holds for $m = 0, \dots, M-2$. Then*

$$|\mathbb{E}[\Phi(X(T))] - \mathbb{E}[\Phi(X^h(T))]| \leq Th C_{\text{weak}}^{\text{rec}}(T, W) + C_{\text{term}}(T)h,$$

where

$$C_{\text{weak}}^{\text{rec}}(T, W) = C_{\text{diff}}(T) + \frac{M_I(T)}{\tau_c} R_{\text{net}}(T)\|W\|_1 + \frac{M_v(T)}{2} \sum_{i=1}^{N_r} \rho_{\text{max},i}^V(T) A_{2,i}(T) + \|u\|_\infty R_{\text{net},2}(T),$$

and $C_{\text{term}}(T)$ controls the final step $m = M-1$ (where transmission at $t = T$ need not hold). If Φ is spike-map compatible at T , one may take $C_{\text{term}}(T) = 0$.

Proof. Use the telescoping identity $\mathbb{E}[\Phi(X(T))] - \mathbb{E}[\Phi(X^h(T))] = \sum_{m=0}^{M-1} \mathbb{E}[u(t_{m+1}, X_{m+1}^h) - u(t_m, X_m^h)]$, apply Lemma 7.1 to $m \leq M-2$ and bound the last step by $C_{\text{term}}(T)h$. \square

Remark 7.3 (Effect of bursty synchrony). The bursty synchronous regime corresponds to large $R_{\text{net}}(T)$ and $R_{\text{net},2}(T)$. The weak order remains 1 under these bounds, but the constants can become large. Moreover, synchronized regimes can increase the strip-density constants $\rho_{\text{max},i}^V(T)$ and the velocity moments $A_{2,i}(T)$ (in small-noise limits these may blow up), further increasing $C_{\text{weak}}^{\text{rec}}(T, W)$.

8 Discussion

The numerical phenomena studied in this manuscript are closely tied to how spiking networks are used. For neuroscience modeling, the strong results quantify when a time-driven scheme reproduces individual spike trains over finite horizons, and the weak results quantify when it reproduces smooth readouts such as firing-rate-dependent functionals. These are different accuracy notions because the threshold/reset rule is discontinuous: a small subthreshold state error can translate into an $O(1)$ change in a spike count or in a terminal discontinuous observable. Our analysis makes this separation explicit by isolating spike-time error, transversality at threshold, and terminal mismatch events.

From a modeling perspective, the transversality variable $A = I - I_{\text{th}}$ has a direct interpretation. Large A corresponds to robust threshold crossings, while small A corresponds to fluctuation-driven, nearly tangential spikes that are intrinsically harder to resolve on a grid. The logarithmic inverse-moment bound shows that, under a boundary-flux control, these difficult crossings are rare enough that the good-set mean-square error remains h up to polylogarithmic factors. In other words, the classical Euler–Maruyama $1/2$ strong behavior survives in the bulk, but resets leave a measurable numerical signature through threshold geometry. This is especially relevant for cortical regimes in which irregular spiking and weakly driven threshold crossings are part of the modeled phenomenon rather than a nuisance [6, 12].

The same conclusions matter for neuromorphic computation and spike-based AI. Many spiking architectures rely on precise event timing, synaptic filtering, and recurrent amplification to process temporal streams or to support online learning [11, 24, 25]. Our bounds suggest a practical distinction: if the task is driven by smooth readouts, order-one weak accuracy may already be adequate, whereas tasks that depend on single-trial timing, causal credit assignment, or spike-triggered updates require control of strong error and of terminal mismatch probabilities. The feedforward result that depth need not change the strong h -exponent, provided no new small-speed events are created downstream, also supports a useful design principle: synaptic depth can amplify constants without necessarily changing the basic discretization scaling.

Below we mention several important extensions.

On the modeling side, conductance-based synapses, adaptation currents, heterogeneous delays, and plasticity rules would move the theory closer to contemporary neuroscience models and to hardware spiking systems [11, 12, 17]. On the numerical side, the present estimates point directly toward adaptive or event-corrected schemes that refine only near threshold, namely in the regime where the transversality variable is small and time-driven Euler–Maruyama is intrinsically most fragile. A second priority is to connect the present pathwise theory to population-level PDE and statistical-mechanics descriptions. Our constants depend on two density objects: the threshold flux, which controls near-tangential crossings, and the voltage mass in a strip below threshold, which controls false positives and weak defects. In asynchronous regimes these quantities are often regular enough to be estimated from mean-field or Fokker–Planck descriptions, whereas in synchronized or strongly self-excitatory regimes the same descriptions can develop sharp boundary layers and even collective firing singularities [7, 8, 10, 16]. Bringing such PDE estimates back into the pruning argument could turn qualitative rate/density assumptions into quantitative functions of noise level, coupling strength, and E–I balance, and would connect the present numerical analysis more directly to the statistical mechanics of spiking populations [3, 29, 30].

The main mathematical limitation of the current strong theory is that it treats T and L as fixed and uses a deliberately conservative recursion. Once an upstream spike-time error appears, the bound passes its maximal downstream impact forward through all later layers. This is robust for finite T and L , but it ignores spike causality. A perturbation in layer 1 changes the current in layer 2 immediately, yet it can alter spike times in deep layers only through a cascade of later threshold crossings. Thus, for large depth or long time, the relevant object is not an

instantaneous all-to-all transfer of the upstream supremum error, but a causal genealogy of descendant spikes. A sharper strong-error theory should therefore replace the present layerwise max recursion by a causal Green’s-function or Volterra representation for the hybrid variational equation. One natural target would be an estimate of the form

$$\Delta_\ell(t) \lesssim \text{Loc}_\ell(t) + \sum_{m < \ell} \int_0^t G_{\ell m}(t, s) \Delta_m(s) dN_m(s) + \text{Prune}_\ell(t),$$

where $G_{\ell m}(t, s)$ is a path-sum kernel built from synaptic filters, weights, and saltation factors along directed causal chains. Such a representation would discount layers that have not yet been reached by a spike cascade and would replace the raw depth L by the size of an effective causal cone. If the integrated gain operator has spectral radius below one, or more generally if the hybrid dynamics is contracting on average, one could hope for strong bounds that are uniform in T and sublinear in L , or even uniform in both after the initial transient. For recurrent networks, the same idea becomes a loop expansion over directed cycles, weighted by path length and cycle length, and may substantially sharpen the current gain-matrix truncation.

For weak error, the long-time and large-depth problem should also be reformulated. The present $O(Th)$ estimate is obtained by summing one-step defects over time, which is appropriate on finite horizons but not optimal as $T \rightarrow \infty$. A more natural route is to use the hybrid Markov semigroup and solve a Poisson equation for the centered observable,

$$\mathcal{L}u = \Phi - \pi(\Phi),$$

with π an invariant law. If the exact and numerical chains are geometrically mixing and the boundary-strip terms are integrable under π , one may hope to replace linear growth in T by a uniform-in-time $O(h)$ bias after an initial relaxation period. An analogous idea applies in depth: instead of accumulating weak defects layer by layer, one can study a transfer operator in the layer index and ask whether local perturbations decay as they propagate through balanced feedforward structure. Under suitable balance or dissipation assumptions, the weak defect at a readout layer should depend on the response of the associated transfer operator rather than on the full depth L itself. In a simultaneous large-population limit, the resulting constants could then be expressed through stationary McKean–Vlasov or Fokker–Planck quantities, linking numerical error for finite-network simulation to the macroscopic order parameters and correlation structure studied in statistical mechanics [3, 29, 30].

Finally, an important direction is to go beyond absorbing couplings. The current pruning argument is intentionally one-sided: once an exact and numerical path mismatch, the path is discarded. For long times this is likely too pessimistic. The Lyapunov analysis suggests that in contracting regimes trajectories may re-synchronize after a transient mismatch, especially when the mismatch does not trigger a persistent difference in downstream spike cascades. Constructing non-absorbing couplings that allow such recovery would preserve the interpretability of the present theory while potentially yielding much sharper long-time strong bounds. This appears to be the right framework for connecting numerical analysis, dynamical stability, and statistical mechanics in large spiking neural networks.

References

- [1] B. BOUCHARD, S. GEISS, AND E. GOBET, *First time to exit of a continuous Itô process: General moment estimates and L^1 -convergence rate for discrete time approximations*, Bernoulli, 23 (2017), pp. 1638–1682.
- [2] B. BOUCHARD AND S. MENOZZI, *Strong approximations of BSDEs in a domain*, Bernoulli, 15 (2009), pp. 1136–1177.

- [3] P. C. BRESSLOFF, *Stochastic neural field theory and the system-size expansion*, SIAM Journal on Applied Mathematics, 70 (2010), pp. 1488–1521.
- [4] R. BRETTE, *Dynamics of one-dimensional spiking neuron models*, Journal of Mathematical Biology, 48 (2004), pp. 38–56.
- [5] R. BRETTE AND E. GUIGON, *Reliability of spike timing is a general property of spiking model neurons*, Neural Computation, 15 (2003), pp. 279–308.
- [6] R. BRETTE, M. RUDOLPH, T. CARNEVALE, M. HINES, D. BEEMAN, J. M. BOWER, ET AL., *Simulation of networks of spiking neurons: A review of tools and strategies*, Journal of Computational Neuroscience, 23 (2007), pp. 349–398.
- [7] N. BRUNEL, *Dynamics of sparsely connected networks of excitatory and inhibitory spiking neurons*, Journal of Computational Neuroscience, 8 (2000), pp. 183–208.
- [8] M. J. CÁCERES, J. A. CARRILLO, AND B. PERTHAME, *Analysis of nonlinear noisy integrate & fire neuron models: Blow-up and steady states*, Journal of Mathematical Neuroscience, 1 (2011).
- [9] M. DAVIES, N. SRINIVASA, T. LIN, G. CHINYA, Y. CAO, S. H. CHODAY, G. DIMOU, P. JOSHI, N. IMAM, S. JAIN, Y. LIAO, C. LIN, A. LINES, R. LIU, D. MATHAIKUTTY, S. MCCOY, A. PAUL, J. TSE, G. VENKATARAMANAN, Y. WENG, A. WILD, Y. YANG, AND H. WANG, *Loihi: A neuromorphic manycore processor with on-chip learning*, IEEE Micro, 38 (2018), pp. 82–99.
- [10] F. DELARUE, J. INGLIS, S. RUBENTHALER, AND E. TANRÉ, *Global solvability of a networked integrate-and-fire model of mckean-vaslov type*, The Annals of Applied Probability, 25 (2015), pp. 2096–2133.
- [11] J. K. ESHRAGHIAN, M. WARD, E. O. NEFTCI, X. WANG, G. LENZ, G. DWIVEDI, M. BENNAMOUN, D. S. JEONG, AND W. D. LU, *Training spiking neural networks using lessons from deep learning*, Proceedings of the IEEE, 111 (2023), pp. 1016–1054.
- [12] W. GERSTNER, W. M. KISTLER, R. NAUD, AND L. PANINSKI, *Neuronal Dynamics: From Single Neurons to Networks and Models of Cognition*, Cambridge University Press, Cambridge, 2014.
- [13] E. GOBET, *Weak approximation of killed diffusion using Euler schemes*, Stochastic Processes and their Applications, 87 (2000), pp. 167–197.
- [14] D. HANSEL, G. MATO, C. MEUNIER, AND L. NELTNER, *On numerical simulations of integrate-and-fire neural networks*, Neural Computation, 10 (1998), pp. 467–483.
- [15] A. HANUSCHKIN, S. KUNKEL, M. HELIAS, A. MORRISON, AND M. DIESMANN, *A general and efficient method for incorporating precise spike times in globally time-driven simulations*, Frontiers in Neuroinformatics, 4 (2010), p. 113.
- [16] J. HU, J.-G. LIU, Y. XIE, AND Z. ZHOU, *A structure preserving numerical scheme for Fokker–Planck equations of neuron networks: Numerical analysis and exploration*, Journal of Computational Physics, 433 (2021), p. 110195.
- [17] G. INDIVERI, B. LINARES-BARRANCO, T. J. HAMILTON, A. VAN SCHAİK, R. ETIENNE-CUMMINGS, T. DELBRUCK, S.-C. LIU, P. DUDEK, P. H^o AFLIGER, S. RENAUD, J. SCHEM-MEL, G. CAUWENBERGHS, J. ARTHUR, K. HYNNA, F. FOLOWOSELE, S. SA^oIGHI, T. SERRANO-GOTARREDONA, J. WIJEKON, Y. WANG, AND K. BOAHEN, *Neuromorphic silicon neuron circuits*, Frontiers in Neuroscience, 5 (2011), p. 73.

- [18] G. INDIVERI AND S. LIU, *Memory and information processing in neuromorphic systems*, Proceedings of the IEEE, 103 (2015), pp. 1379–1397.
- [19] P. E. KLOEDEN AND E. PLATEN, *Numerical Solution of Stochastic Differential Equations*, Springer, 1992.
- [20] W. MAASS, *Networks of spiking neurons: The third generation of neural network models*, Neural Networks, 10 (1997), pp. 1659–1671.
- [21] C. A. MEAD, *Neuromorphic electronic systems*, Proceedings of the IEEE, 78 (1990), pp. 1629–1636.
- [22] P. A. MEROLLA, J. V. ARTHUR, R. ALVAREZ-ICAZA, A. S. CASSIDY, J. SAWADA, F. AKOPYAN, B. L. JACKSON, N. IMAM, C. GUO, Y. NAKAMURA, B. BREZZO, I. VO, S. K. ESSER, R. APPUSWAMY, B. TABA, A. AMIR, M. D. FLICKNER, W. P. RISK, R. MANOHAR, AND D. S. MODHA, *A million spiking-neuron integrated circuit with a scalable communication network and interface*, Science, 345 (2014), pp. 668–673.
- [23] A. MORRISON, S. STRAUBE, H. E. PLESSER, AND M. DIESMANN, *Exact subthreshold integration with continuous spike times in discrete-time neural network simulations*, Neural Computation, 19 (2007), pp. 47–79.
- [24] E. O. NEFTCI, H. MOSTAFA, AND F. ZENKE, *Surrogate gradient learning in spiking neural networks: Bringing the power of gradient-based optimization to spiking neural networks*, IEEE Signal Processing Magazine, 36 (2019), pp. 51–63.
- [25] K. ROY, A. JAISWAL, AND P. PANDA, *Towards spike-based machine intelligence with neuromorphic computing*, Nature, 575 (2019), pp. 607–617.
- [26] C. D. SCHUMAN, S. R. KULKARNI, M. PARSA, J. P. MITCHELL, P. DATE, AND B. KAY, *Opportunities for neuromorphic computing algorithms and applications*, Nature Computational Science, 2 (2022), pp. 10–19.
- [27] M. J. SHELLEY AND L. TAO, *Efficient and accurate time-stepping schemes for integrate-and-fire neuronal networks*, Journal of Computational Neuroscience, 11 (2001), pp. 111–119.
- [28] J. TERAMAE AND D. TANAKA, *Robustness of the noise-induced phase synchronization in a general class of limit cycle oscillators*, Physical Review Letters, 93 (2004), p. 204103.
- [29] J. TOUBOUL, *Propagation of chaos in neural fields*, The Annals of Applied Probability, 24 (2014), pp. 1298–1328.
- [30] J. D. TOUBOUL AND G. B. ERMENTROUT, *Finite-size and correlation-induced effects in mean-field dynamics*, Journal of Computational Neuroscience, 31 (2011), pp. 453–484.